Numerical optimization and convective thermal loss analysis of improved solar parabolic trough collector receiver system with one sided thermal insulation

A Dissertation submitted
in partial fulfillment of the requirements
for the degree of

Master of Engineering (M.E.)

In

Thermal Engineering

By

Yogender Pal Chandra
Registration No.: 801483026

Under supervision of

Dr. J.P. Kesari
Associate Professor
Department of Mechanical Engineering
Delhi Technological University (DTU),
Delhi – 110042

Dr. S.K. Mohapatra
Senior Professor and Head
Mechanical Engineering Department
Thapar University, Patiala
Punjab

MECHANICAL ENGINEERING DEPARTMENT

THAPAR UNIVERSITY, PATIALA

July, 2016

CERTIFICATE

I hereby declare that the thesis entitled, "**Numerical optimization and convective thermal loss analysis of improved solar parabolic trough collector receiver system with one sided thermal insulation**" is an authentic record of my work carried out in requirements for the award of the degree of **Master of Engineering** in **Thermal Engineering** at **Thapar University**, **Patiala**, under the supervision of **Dr. S.K. Mohapatra**, **Senior Professor and Head of Department, Mechanical Engineering Department**, **Thapar University**, **Patiala** and **Dr. J.P. Kesari, Associate Professor, Department of Mechanical Engineering, Delhi Technological University (DTU), Delhi** during July, 2014 to July 2016. No part of the matter embodied in this report has been submitted to any other university or institute for the award of any degree.

Date: 10/07/2016

Yogender Pal Chandra

It is certified that the above statement made by the student is correct to the best of my/our knowledge and belief.

Dr. J.P. Kesari
Associate Professor
Department of Mechanical Engineering
Delhi Technological University (DTU),
Delhi – 110042

Dr. S.K. Mohapatra
Senior Professor and Head
Mechanical Engineering Department
Thapar University
Patiala-147004, Punjab

Countersigned by

Head, Mechanical Engineering Department
Thapar University, Patiala - 147004

Dean of Academic Affairs
Thapar University, Patiala - 147004

In memory of

Late Smt. Indra Chandra

You left fingerprints and trace of grace on my life…

You shan't be forgotten…

Dedicated to

Dear Papa,

You came upon me craving some kind of little figure out of wood and you said," why don't you make something for me?"

I asked you what you wanted and you said, "A box."

"What for?"

"To put things in."

"What kind of things?"

"Whatever you have," you said.

Well, here's your box. Nearly everything I have is in it, and it is not full. Pain and excitement are in it, feeling good or bad, evil thoughts and good thoughts, pleasure and despair and the indescribable joy of creating this thesis work. Most importantly, and above all, the gratitude and love I have for you.

And still box in not full!

Bittoo.

Acknowledgments

I would like to express my deepest gratitude to Professor Dr. S.K. Mohapatra and Dr. J.P. Kesari, my research supervisors, for their excellent guidance, enthusiastic encouragement, useful critiques and providing me with an excellent atmosphere for doing research. Your advice on both research as well as on my career have been priceless.

The opportunity, support, exposure and atmosphere provided by the Thapar University, Patiala, to incubate my future is highly appreciated. The financial support provided by the All India Council of Technical Education (AICTE) to carry out my studies is greatly appreciated.

A special debt of gratitude is owed to the authors whose works I have consulted and quoted in this work.

Last but not least, I am forever grateful to my parents, family and friends for their unconditional support and best wishes.

Yogender Pal Chandra

ABSTRACT

Two types of receiver systems currently employed in solar parabolic trough collector technology are evacuated annuli receivers and air filled annuli receivers. While former receiver find its way into high temperature grid-acquaintance solar parabolic trough collectors, latter are more inclined towards non-grid solar thermal applications like low temperature process heat. Evacuated receivers utilize vacuum filled annuli to stamp down the convection losses; this makes them substantially expensive—while prizing them with benchmark among receivers. Contrary, air filled annuli based receivers are relatively less expensive, but are subpar in thermal performance relative to evacuated receivers. This work deals with the air filled receiver system and would try to abridge the economy and efficiency between both types of system using computational fluid dynamics based numerical simulation approach. A heat blocking thermal insulator is jibed in the sun facing receiver annulus, which does not receive concentrated Sun's radiation, and is simulated for the combined conduction and convective losses and also for better temperature distribution around the absorber. Consequently, its convective heat losses were investigated for varying wind speed and mass flow rate of heat transfer fluid and are compared with mainstream air filled annuli receivers. Simulation results are compared with experimentation in which wind velocity was in range of 0.43 – 4.99 m/s, glass envelop temperature decreased with increase in wind velocity which directly insinuates the decrease in convection losses around glass envelop. These comparative implications could be served as a point of reference par excellence to develop solar parabolic trough collector for small scale process heat applications in India.

Keywords: Parabolic trough collector; air filled annulus receiver; convective heat loss; computational fluid dynamics.

TABLE OF CONTENTS

LIST OF FIGURES

LIST OF TABLES

Nomenclature

A = Inner diameter of absorber

a = Aperture

A_c = Net area of solar collector

$C_{p\text{-}f}$ = Specific heat at constant pressure

D_2 = Outer diameter of glass envelop

$d_{g\text{-}i}$ = Inner diameter of glass tube

$d_{g\text{-}o}$ = Outer diameter of glass tube

$d_{r\text{-}o}$ = Outer diameter of absorber

f = Focal length of mirror

G_b = Kinetic energy generation due to buoyancy effect

G_k = Kinetic energy generation due to turbulent flow

$h_{a\text{-}g}$ = Convective heat coefficient for the trapped air in annulus

h_w = Convective heat transfer coefficient of wind

I_b = Solar heat influx on collector

I_{sc} = Solar constant

k = Turbulent energy production

k_e/k = Equivalent thermal conductivity ratio

k_e = Thermal conductivity of stationary fluid for same heat transfer rate

k_T = Turbulent conductivity

$Nu_{g\text{-}a}$ = Nusselt number for air over glass

$Q_{a,f\text{-}conv}$ = Convective heat transfer from fluid

Q_c = Net heat transfer

$Q_{g\text{-}conv}$ = Convective heat loss from glass tube

Q_u = Net heat transfer in HTF

$q_{a\text{-}conv}$ = Buoyancy induced convection

$q_{a,f\text{-}conv}$ = Heat transfer from absorber to HTF *via.* convection

$q_{g\text{-}conv}$ = Convection through glass tube

q_{sol} = Solar heat influx in lower part of receiver

$q_{sol\text{-}abs}$ = Solar radiation transmitted to absorber after passing through glass

Ra_m = Modified Rayleigh number

R_e = Reynolds number

T_g = Glass temperature

T_∞ = Ambient temperature

U_c = Heat loss coefficient

V_w = Velocity of air

V_f = Velocity of fluid

T_a = Absorber temperature

T_c = Collector temperature

T_f = Temperature of fluid

Greek Symbols

α = Altitude angle

γ = Surface azimuth angle

δ = Declination angle

ε = Turbulent energy dissipation

ε_e = Surface emissivity

ε_w = Transmittance

η_o = Optical efficiency

θ = Zenith angle

θ_i = Incidence angle

λ_{g-a} = Thermal conductivity of air

λ_{eff} = Effective conductivity of trapped air in annulus

μ_t = Turbulent viscosity or eddy viscosity

ρ_f = Fluid viscosity

σ = Stefan-Boltzmann constant

ϕ = Latitude angle

φ = Circumferential angle of receiver

ω = Hour angle

Acronyms

BS = Backup storage

BPO = Biphenyl/Dyphenyl oxide

CFD = Computational fluid dynamics

CLFR = Compact linear Fresnel reflector

CSP = Concentrating solar power

CST = Concentrated solar thermal

CTD = Circumferential temperature difference

PTC = Parabolic trough collector

DNI = Direct normal irradiance

DSG = Direct steam generation

LFR = Linear fresnel collector

FVM = Finite volume method

GC = Geometric concentration

HFC = Heliostats field collector

HTF = Heat transfer fluid

LCOE = Levelized cost of energy

MCRT = Monte-Carlo ray trace

NISE = National Institute of Solar Energy

Nu = Nusselt number

PCM = Phase change material

PDC = Parabolic dish concentrator

PDE = Partial differential equation

RTD = Resistance temperature detector

SPV = Solar photovoltaic

SRT = Solar ray tracing

S2S = Surface to surface

TES = Thermal energy storage

CHAPTER 1

INTRODUCTION AND OBJECTIVES

1.1 Introduction

With depleting state of fossil fuels, there immerges a considerably great need of affordable and clean source of energy with the view to satisfy the already overgrown energy demands. Correspondingly, with the intensified energy demands, which actually happened within a decade or so, achieving sustainable supply for the future has become a great challenge. As a matter of fact, sunlight provides greater amount of energy in 1 hour then actually it is being consumed on the planet in whole whopping 1 year. All the same, only fraction of the world's total power consumption comes from solar energy. To begin with, there comes two vogue class of technologies used to conserve the solar energy namely concentrated solar power (CSP) and photovoltaic (PV). While, the latter employs the use of solar photovoltaic cells to produce electricity *via.* photoelectric effect, the former employs various methods of heat capturing devices and structures and finally using that thermal energy into some power producing thermal cycles, more preferably Rankine cycle.

Concentrated solar power (CSP) has been a subject of great interest worldwide for several decades with Spain in its leading rein [Antonelli et al., 2015]. Concentrating solar energy employs a complicated scheme of mirrors with a sun tracking arrangement, heat transfer fluids to transport the necessary thermal energy to the power block where it can be fed to power turbine to generate electricity *via*. some power cycle, Rankine cycle more preferably. Four primary types of solar collectors can be differentiated, with chief among these technologies include parabolic trough collector (PTC), linear fresnel reflector (LFR), heliostats field collector (HFC) and concentrated dish sterling or parabolic dish concentrator (PDC).

Solar energy being very sparse cannot produce necessary heating affects as such on its own, henceforth, it is quite indispensible to concentrate it on a point or a line from where heat could be taken of *via.* heat transfer fluids. Thus, giving it a unique form of peculiarity among PTC and HFC. To illustrate, linear concentration technology of parabolic trough collectors has taken CSP by storm: there is no definitive focusing point, rather a line. Serious development and evolution of this technology, in fact, came into existence when scientists analyzed step by step and wrap by wrap, the existing forefront point focusing technology and

suddenly stumbled upon a common notion – why, point concentrate the heat? When it will be redistributed anyways, in line circuitry of the heat transfer fluid. Parabolic trough based concentrated solar thermal power plants, for the most part consists of parabolic trough solar fields, heat generation system or absorber/receiver system, power block powered with Rankine steam turbine and a temporary or optional power storage system. This work will try to put direct contrast on each of the concentrated solar power (CSP) technologies with reviewing prominent areas of its working such as solar collector design and materials, heat transfer mechanism with various methods employed by heat transfer fluids (HTF), decisive factors which are very critical for choosing HTF whether it is direct steam generation (DSG); liquid salt heat transport system or some other thermal oil based heat transfer system. Finally, thermal storage systems and its efficacies would be considered as a comprehensive review.

The central gist of this work would not only address the problem thus formulated; which is actually conceptualised overleaf, however, could be most significantly digressed towards the application of CSP technology which actually offer a diverse variety of application for which concentrated solar thermal energy can be put into service. Chief among these services other than power production includes salt water desalination, industrial process heat, chemical production, heating and cooling of conditioned space and so on and so forth. Concentrated solar thermal (CST) energy finds its application worthwhile in clean water scarce regions around the world which definitely have high solar flux insolation. In another words, salt water desalination compounded with CST could be employed to purify salt water which require huge amount of energy to evaporate the water from salt water mixture and consequently condensing the same pure water for portability and agricultural purpose. Henceforth, CST energy seems to be most suited technology for the regions of low water and electricity availability. In conclusion, a great many variety of application for a good cause can be unified with CSP technology provided a sincere investment in terms of research, investment and public acceptability is associated with it.

To quantify the introductory phase and before heading towards literature review, de facto, India having high solar insolation is very ideal place for solar electricity generation *via.* CSP or photovoltaic. Quite recently, a 35000 km^2 area of Thar dessert is proposed for large solar power projects, to generate around 2100 GW of power. Today, among 38,283.59 MW of total installed capacity around 4,684.74 MW of electricity is generated by solar projects. Which is around 12% of the total installed capacity. As a matter of fact, India is expected to install an additional 10,000 MW by 2017 and a total of 100,000 MW by 2022. Currently, the French group AREVA solar is constructing and installing a 250 MW CSP plant that has

actually grounded a milestone in Rajasthan being largest CSP installation in Asia this far. Breathtakingly, Mega Green Solar Power Projects is also planning and installing a whopping 4000 MW solar project near Sambhar Lake in Rajasthan. Once it is completed, it would be biggest solar project on the planet.

1.2 Objectives

Addressing aforementioned glitches in the working of conventional air filled annuli receivers, ensuing objectives are toiled upon, to;

- Simulate and study the temperature distribution of conventional air filled annulus PTC receiver which is being commissioned at National Institute of Solar Energy (NISE), Gurgaon, Haryana;
- Simulate and study temperature distribution of proposed reformed and modified receiver, while, comparing it with the conventional one;
- Study comparative heat loss in both the receivers, with varying thermo – physical properties.

CHAPTER 2

LITERATURE REVIEW

This chapter demonstrates the congenial research work conveyed by scholars and researchers on solar parabolic trough collectors and heat interaction analysis of the receiver. The preliminary part of this chapter is dedicated to broad – spectrum concepts on a solar thermal process and related models. Finally, in subsequent sections, different heat transfer model presented by various researches are illustrated.

2.1 Sun intensity

The energy emitted by sun is in the form of electromagnetic radiation. These radiations are of almost all wavelengths occurring in between infrared radiation, ultraviolet radiation and the visible light. By the previous results it has been calculated that the effective temperature of the sun is 5762 K. It behaves as a source of energy due to continuous chain reaction happening there in the atmosphere of sun. The energy transmitted by the sun can be calculated by the Stefan-Boltzmann law, which states:

$$E=\varepsilon\sigma T^4 \tag{2.1}$$

Where,

ε = Surface Emissivity, σ = Stefan – Boltzmann constant

48% of the Sun's radiation reaching the Earth surface falls in visible spectrum, while, 45.6% in infrared spectrum and the finally the remaining 6.4% in ultraviolet region.

2.2 Diffuse and direct solar radiation

Some part of the Sun's radiation falling in ultraviolet spectrum gets absorbed by ozone layer, while some part falling in infrared spectrum gets absorbed by the water vapour, and CO_2 present in the atmosphere. So the effective intensity of Sun's radiation reaching the earth surface gets mitigated to a substantial value. These radiations can be categorised in two ways depending upon the following criteria.

2.3 Diffuse solar radiation

Diffuse radiation, skylight, diffuse skylight, or sky radiation is the solar radiation which reaches the earth surface after getting scattered by the molecules, water vapour and suspensions present in earth atmosphere

2.4 Direct (beam) solar radiation

If the radiation reaches the earth surface without getting diffused, it is referred as direct solar radiations. Depending upon the weather condition it can be decreased by 100% on the rainy or cloudy day. Direct radiation is also termed as solar intensity in common jargon. To have an average value of intensity throughout year, solar constant I_{sc} is calculated, and its average value is taken as 1367 W/m^2.

2.5. Material interaction with solar radiation

Solar radiation striking on any material, interact with it in three possible ways, namely:

- Reflected radiation (G_r)
- Absorbed radiation (G_a)
- Transmitted radiation (G_t)

$$G_{total} = G_r + G_t + G_a$$

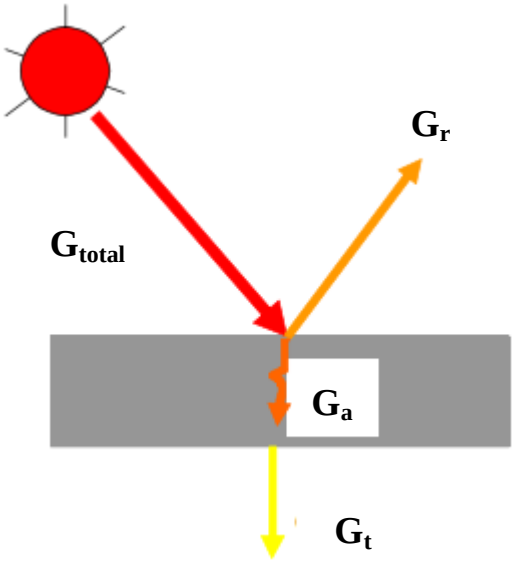

Figure 2.1 Material interaction of solar beam.

2.6 The Sun and the Earth angles

The following are the important Sun – Earth angles:

Zenith angle (θ): The angle traced between ray of the sun and the perpendicular to horizontal

plane is named as Zenith angle.

Altitude angle (α): Contrary to zenith angle it is the angle traced between Sun's ray and horizontal plane.

Surface azimuth angle (γ): Surface azimuth angle is actually traced in the horizontal plane, in contrast to the other two planes, it is the angle traced by projection of suns ray in the horizontal plane and the line pointing south.

Latitude (ϕ): Any location is spotted by two set of numbers namely longitude and latitude. If the angle traced by circumferential line which actually passes through that location and head towards the centre of the earth to its projection on equatorial plane.

Declination (δ): Declination angle is defined as the angle traced between the line joining centre to centre distance of earth and sun and its plan on equatorial plane.

Hour angle (ω): It is defined as the angle that earth should be rotated to bring its meridian under the sun.

Angle of incidence (θ_i): Angle of incidence is reckoned out with the beam radiation onto the surface tracing the angle with normal to surface.

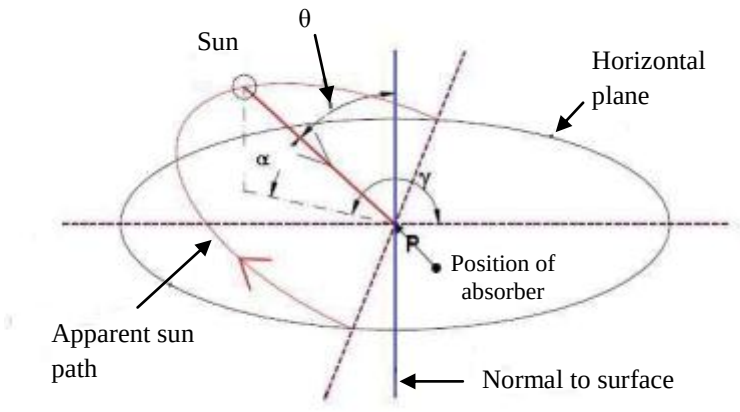

Figure 2.2 Different Earth angles [Antonellie et al., 2015]

2.7 Applications of solar energy

Following are the application areas of the solar energy.

- Process heating
- Electricity/Power generation
- Cooling and refrigeration
- Agriculture and horticulture in form of solar driven irrigation pump
- Cooking/Process heating

- Drying/Timber seasoning

Schematics of some major solar applications are shown in subsequent fig. 2.3

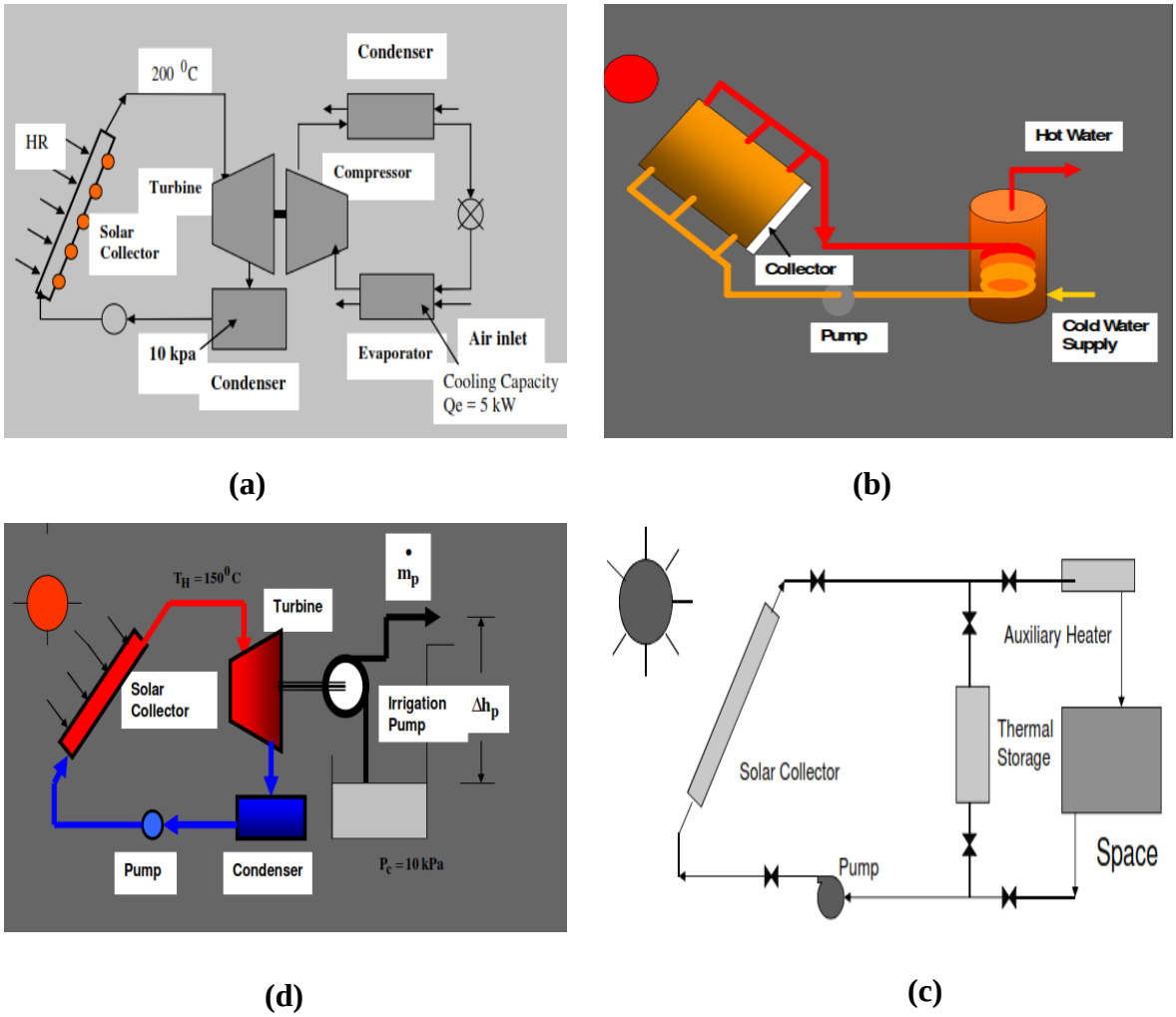

Figure 2.3 Schematic of (a) solar cooling system, (b) solar water heater, (c) solar irrigation system, and (d) solar space heating

Solar energy could be used directly rather, through PV cells, where radiation can be directly converted into DC electricity and this energy can be stored in the battery to use in night or in the cloudy day.

Solar photovoltaic (SPV) has a large number of applications, which includes:

- Domestic lighting
- Street lighting in villages and townships
- Electrification
- Water pumping
- Desalination of salty water

- Powering to remote telecommunication repeater stations and railway signals.

2.8 Solar collectors

These are the devices which are used to collect the solar irradiations, and by some means transfer that energy to some working fluid, through which thermal energy can be made to used.

Primarily two categories are considered; with chief among them includes:

- Non – concentrating solar collectors
- Concentrating solar collectors

2.9 Non – concentrating type solar collectors

2.9.1 Flat plate solar collector

In such collectors both collector and absorber are incorporated into a single entity which is termed as absorber plate in common jargon. These are mostly used for the domestic purpose applications which entail low temperature of working fluid like water heating and food drying.

Basic part of non-concentrating flat plate solar collector includes:

- Absorber plate: With the purpose of absorbing as much heat as it could, absorber plates are made up of extremely high conducting metal.
- Tubes or fins: Heat transfer fluid (HTF) is made to pass through tubes and fins hence conductivity of the metal from which it is made bears paramount importance.
- Glazing: Heat loss prevention is accommodated by a very thin leaf of glass or plastic called glazing.
- Thermal insulation: Heat is prevented from being lost through the joints, end connectors etcetera with the help to thermal insulations such as glass – wool.
- Cover strip: It is used to prevent the setup form unpredictable weather conditions, by surmounting the whole setup.

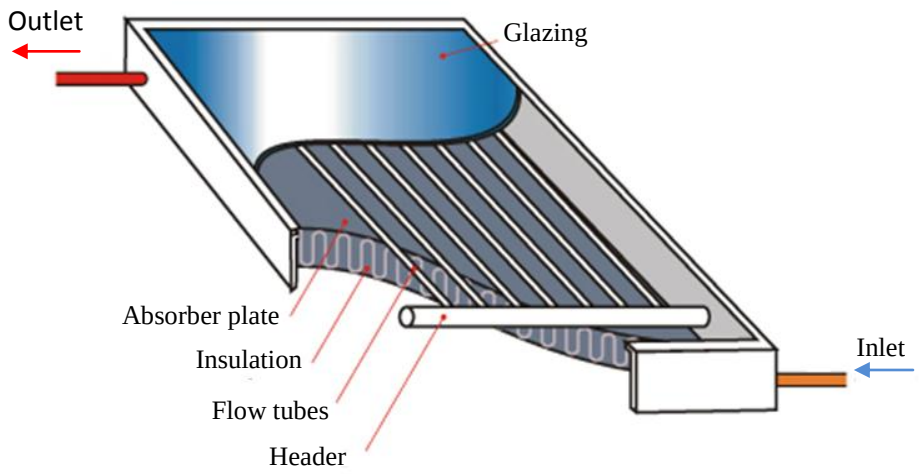

(a)

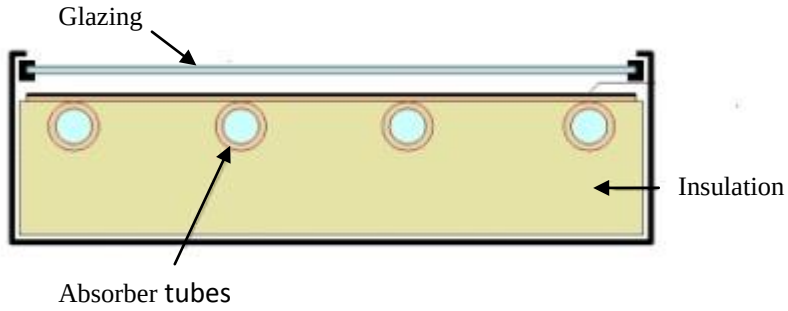

(b)

Figure 2.4 Flat plate collectors for the purpose of domestic water heating (a) 3-D view, and (b) cross sectional view [Antonellie et al., 2015]

Water based non concentrating solar collectors uses water as heat transfer fluid (HTF) for instance, domestic solar water heater (DHW). On the other hand, Air based collector's uses air as HTF, such as air dryer.

Advantages

- It is easy and cheap to fabricate, install, and maintain.
- It can accept both the diffuse and the direct beam solar radiation.
- It does not require sun tracking mechanism.
- It is mechanically much simple as compared to concentrating collectors.
- It can easily attain temperatures in the range of 40 – 70 ^{0}C to heat swimming pools, domestic hot water (DHW), and buildings.

2.9.2 Evacuated tube collector

A number of glass tubes run parallel to each other and each glass tube contains a heat pipe made up of highly conductive material such as copper; this heat pipe serves as an absorber to the system. The glass tube is fabricated in concentric way such that the space between them is vacuumed or evacuated for the sake of convective heat loss reduction. For further reduction of losses, heat pipe material is coated with highly absorptive material with very low reflectivity.

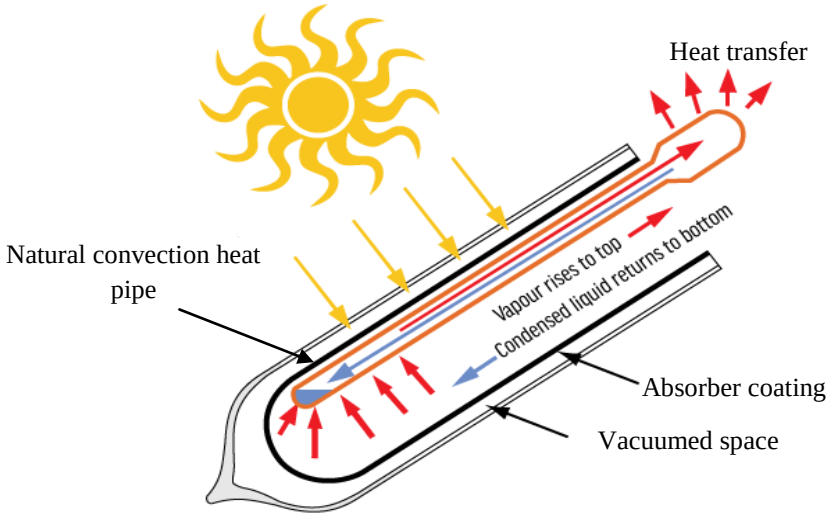

(a)

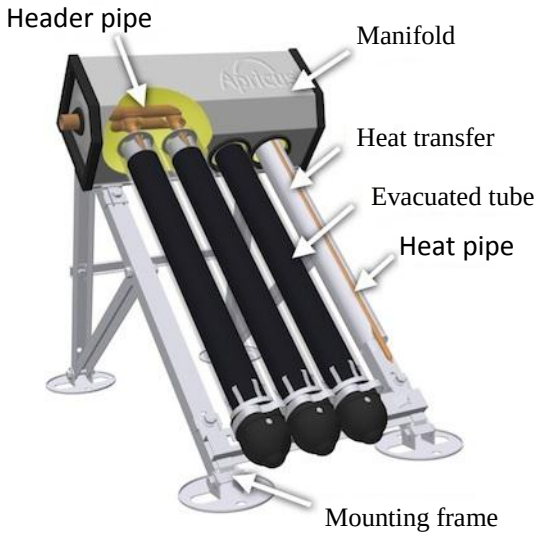

(b)

Figure 2.5 (a) Evacuated tube collector dissection, and (b) a series of evacuate tubes reframed to form domestic solar water heater (DHW) [Antonellie et al., 2015]

Advantages

- Operating temperature of evacuated tube collector is comparatively higher in

contrast to flat plate solar collector.

- Heat losses in evacuated tube collector are far less in contrast to flat plate solar collector.
- Design is very compact and is comparatively cheap.

2.10 Concentrating type solar collector

Intensity of stellar irradiation reaching earth surface is of low quality. However, it can be enhanced by the use of some concentrating methods. So concentrating collector serves to concentrate and intensify solar intensity in a line (line focusing) or a point (point focusing). They can be classified in four ways:

- Parabolic trough collector (PTC)
- Linear fresnel reflector (LFR)
- Power tower or heliostat field collector (HFC)
- Parabolic dish concentrator (PDC)

2.10.1 Parabolic trough collector (PTC)

It's a kind of concentrating solar collector which incorporates a reflecting surface moulded in the shape of parabola, this parabolic shaped collector is fabricated with highly reflecting material which could be highly sophisticated set of mirrors arranged to form a large parabola or some kind of anodized aluminium sheet. On focal length of this huge parabola is situated an absorber/receiver system which collects and welcomes the focused and concentrated radiation coming from the parabolic reflector. This absorber/receiver system conveys high conductive heat transfer fluid. As the solar radiation falls on the parabolic collector, they are being concentrated along a line quite above the parabolic trough, which is generally called as focal length of the parabolic trough. Accordingly, the absorber tube gets heated after some time, and due to its specific property of high thermal conductivity, it transfers its gained heat energy to the heat transfer fluid (HTF) flowing in absorber. Now this heated HTF can be utilised to accomplish the requirement of high temperature. For the absorber, copper or mild steel may be used as a building material. For the better performance, the absorber tube is coated with black colour thermal resistance. By the proper orientation of the parabolic collector towards the Sun, temperature of the heat transfer fluid may rise as high as 400 ^{0}C [Zhang et al., 2013].

Working principle

Parabolic trough collector is most mature solar thermal technology and are generally good

enough for almost all the industrial solar heating applications and a great many of which runs below 400 ^{0}C. PTC collector comprises of a group of mirrors typically made of silver acrylic, set in a tandem and bent into parabolic shape so as to linearly focus all the incident radiation onto the absorber. In another words, many of such sheets are put together to form a long arrays of troughs. The receiver/absorber system which is typically a black metal pipe enclosed in an evacuated glass tube to take care of convection losses, is mounted on the focus of the collector. Vacuum is maintained between the metal pipe and glass tube to minimise the heat losses by convection and radiation. To increase the thermal effectiveness and minimise the losses, an anti-reflective coating is also applied on metal pipe which consequently escalates its transmissivity. Figure 2.6 and fig. 2.7 describes the schematic drawing of PTC with possible heat losses in the receiver [Zhang et al., 2013].

Components

The chief components of parabolic trough solar collector system are

- Reflector**:** The sole purpose of concentrator or reflector is to concentrate the sparse solar radiation falling on it onto the absorber receiver. Typically are made up of highly reflective metal such as silver acrylic, anodised aluminium etcetera.
- Absorber tube: The reflected radiation of higher intensity is concentrated and focused on focal line of parabolic reflector system; this focal line sustains the receiver tube which comprises of concentric glass casing enclosing the absorber tube. This highly conductive tube conveys HTF from which thermal energy is harnessed.
- Glass tube: The absorber tube is surrounded by the glass cover to minimise the losses by, convection and radiation. It has a special property of transparency for the shorter wavelength coming from Sun, and opaque nature to the longer wavelength emitted by the absorber. The spacing in the middle of the glass casing and absorber tube highly affects the performance of the system.
- Support structure: A solid support structure is used to support the trough as wind applies buckling load on the trough. So there is an impending need to support the trough to remain it in the desired position.
- Tracking mechanism: As the position of sun changes, the trough has to manoeuvre its position respective to the Sun’s changing location. This makes sure that full span of radiation is falling on collector aperture every single time. The performance highly depends upon the tracking mechanism of the trough. For efficient tracking,

exceedingly tuned step up motors are put to use.

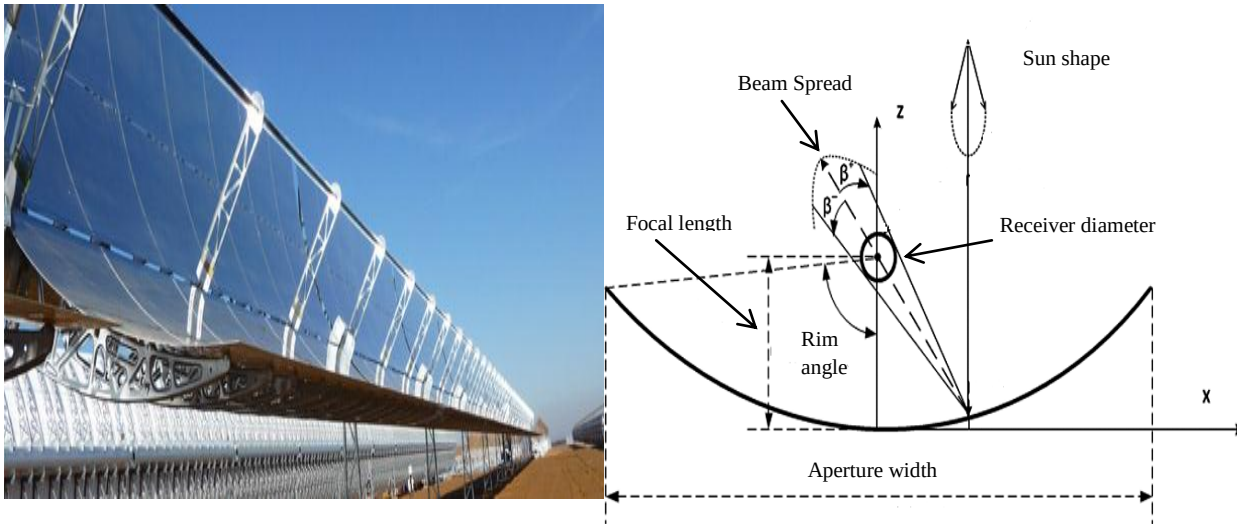

(a) **(b)**

Figure 2.6 (a) Parabolic trough based power plant, Spain (b) geometric design of parabolic trough [Torres solar energy, Spain]

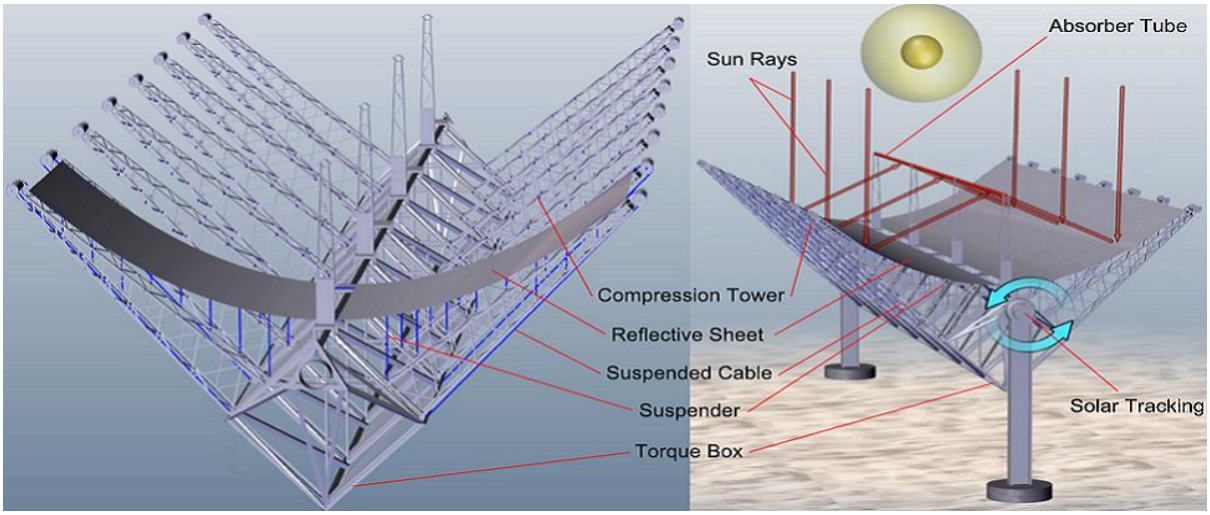

Figure 2.7 General nomenclature of spatial arrangment of PTC
[Torres solar energy, Spain]

Advantages

- It has high efficiency as well as low cost
- Temperatures ranging 150 – 300 ^{0}C can be obtained
- It can be used either for generation of electricity or for thermal energy collection
- Flexible implementation

2.10.2 Linear fresnel reflector (LFR)

LFR and PTC both share the common principle of operation but differ slightly in arrangement. Linear Fresnel reflector is integrated with long arrays of flat mirror which focus the incident solar irradiation onto tower on which receiver is mounted; this tower can be 10 – 15 m tall [Barley et al., 2011]. Contrary to PTC, LFR deploys a great many mirrors arranged in a fashion which approximates the shape of PTC. This makes the LFR design substantially cheaper. In particular, LFR works at lower operating temperature 50 – 300 ^{0}C as compared to PTC (50 – 400 ^{0}C) [Zhang et al., 2013]. The chief benefit of LFR is that it boosts and facilitates direct steam generation hence eliminating any costly secondary heat transfer fluids and heat exchangers. In addition to this, a characteristic challenge with the LFR technology is the shading effect or light blocking effect between the neighbouring reflectors this results to its lack of effectiveness in concentrating Sun's rays onto the receiver [Mills et al., 2000]. Two seemingly possible solution suggested here could be either increase in the mirror spacing, which would eventually add up more land to be required, or increasing the height of the receiver tower which certainly add up cost. A more realistic and innovative solution to the shading problem described above is exemplified by the work of Mills and Morrison in their state of the art scheme of compact linear fresnel reflector (CLFR) [Mills et al., 2000]. This design characterises mirrors arranged towards twin separate mirrors. The use of separate multiple mirrors give a compact reflector distribution and hence reduce the shading effect drastically. Figure 2.8 and fig. 2.9 illustrates the configuration of LFR and CLFR

Advantages

- İt uses flat reflectors instead of complex parabolic shape in case of PTC, which is comparatively cheaper.
- Being mounted near to surface, structural requirements are reduced to a good value resulting still more reduction in cost.

Disadvantages

- A great amount of shading is present in between the neighbouring mirrors which reduces the optical efficiency.
- To reduce the shading affect, inter mirror space is increased which add up the land cost.
- Thermal efficiency is low as compared to parabolic trough collector as it imitates PTC; however, it doesn’t perfectly emulate it.

Figure 2.8 Linear fresnel reflector [Mills et al., 2000]

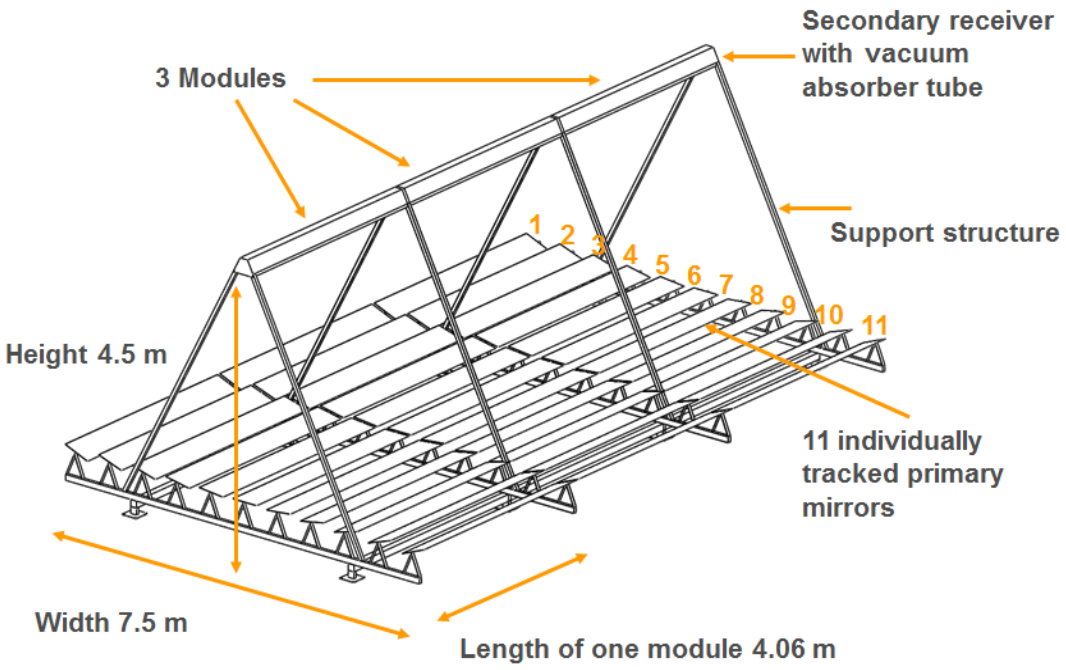

Figure 2.9 Compact linear fresnel reflector (CLFR) [Industrial Solar, Deutschland]

2.10.3 Parabolic dish concentrator (PDC)

Parabolic dish collectors (PDC) are point focusing reflectors reaching concentration ratios of around 1000 Sun and exceeding the operating temperature of about 1500 ^{0}C [Segal et al. 1997]. These high operating parameters make PDC exceedingly forefront technology and demand the service of very efficient power cycles. Essentially, it consists of a large parabolic dish which is mounted on a two axis tracking mechanism which continuously directs all the incident solar radiation onto its focal point. A highly efficient heat engine is mounted on the

focal point of the dish whose sole purpose is conversion of thermal or heat energy to mechanical work. Lastly, an attached alternator converts this heat energy into electricity. Correspondingly, separate unit of reflector, engine and alternator makes fossil fuel hybridization of PDC very facilitating. It is worthwhile to note that PDC does not leave any space to incorporate any thermal storage mechanism. More preferably, below 1000 ^{0}C sterling cycle is used as a heat conversion engine due to its better efficiency below 1000 ^{0}C [Karabulut et al., 2009]. However, at higher temperatures gas turbine cycles usually finds its usage. PDC are highly expensive devices due to their efficacies in working, flawlessness in its concavity and sun tracking tuning. Most importantly, PDC dishes have very small power capacity (usually tens of kW or even smaller) and each dish is responsible of electricity production independently, which do factually means that hundreds of independent dishes would be required to set up a large power producing plant contrary to other CSP technologies. Maricopa Solar Project is the one and only PDC with a capacity of 1.5 MW situated in Arizona, USA [Zhang et al., 2013]. Figure 2.10 depicts the stance of PDC.

Advantages

- Parabolic dishes, as a matter of fact, are highly efficient devices due to the fact that they are facing the sun at every speck of time.
- Ground breaking concentration ratio of about 600 – 2000.
- Being having compact unit of sterling engine compounded with an alternator per dish each dish can work as a single unit or a part of the system of many dishes.

Disadvantages

- A highly tuned up sun tracking mechanism is indispensible for efficient working
- İt is a point focusing collector mainly used in Stirling engines, only for small electricity production.
- Highly costly devices.
- 20 – 30 parabolic dish concentrators are required to be commissioned to build a power plant based on PDC's, as each PDC has its own power producing cycle, hooking up this much of PDC's is pretty difficult task and also ads up a lot of cost to power plant. Henceforth, only one PDC based power plant has been commissioned so far situated in Arizona, USA.

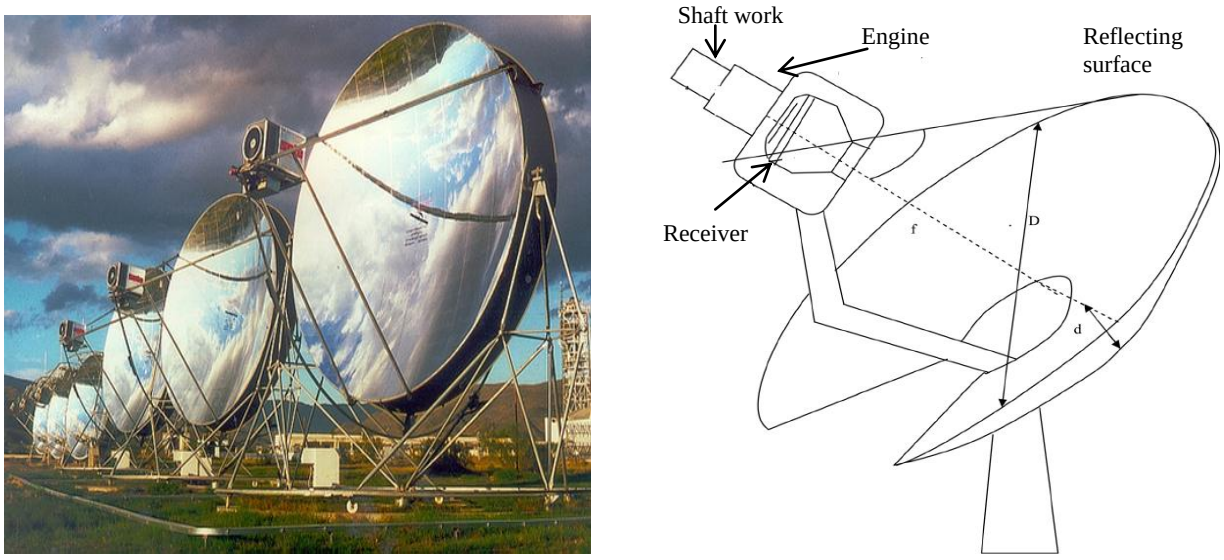

(a) **(b)**

Figure 2.10 (a) parabolic dish collector (PDC) plant, Arizona (b) schematic of PDC [Zhang et al., 2013]

2.10.4 Solar power tower (SPT) or heliostat field collector (HFC)

This is the most recent and '*epoch making'* CSP technology which has found its way into commercial utility and is a boundless success. Heliostat features a scheme of number of flat mirrors spread around the central tower upon which receiver is mounted, this tower is called solar tower in common jargon. Each and every flat mirror or heliostat is mounted on two – axis tracking mechanism to track the sun at every location and has a range of surface area varying from 50 – 150 m^2. Solar tower typically stand tall around 75 – 150 m [Segal et al., 1999]. This much of the height substantially decreases the distance between each mirror and thus saving the land cost and decreasing the shading effect as well. Add – on reward of Heliostat is a significantly large magnitude of solar radiation is concentrated onto the point focus receiver (200 – 1000 kW/m^2), this characteristically intensify the operating temperature (300 – 2000 ^0C). In addition to this, enormous solar radiation focused on the central receiver results a very high concentration ratio (300 - 1500 Suns) Furthermore, this much of the intensified radiation drastically minimizes heat losses thus resulting this much of the operating temperature gain. Heat transport and thermal storage systems are also made simple in solar tower power. Due to very large cost associated with heliostats, STP plants are typically large (10 MW or above) to account for the high cost offsetting. A fluid is made to circulate through the central receiver in a closed loop which is responsible for heat transport for power production or thermal energy storage. Figure 2.11 depicts the stance of solar power tower.

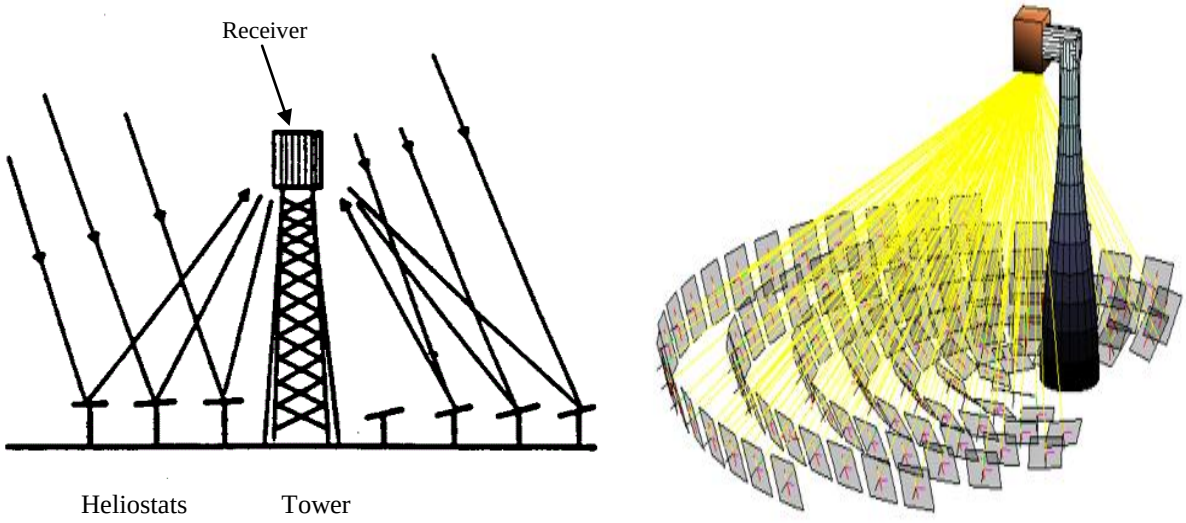

(a) **(b)**

(c)

Figure 2.11 (a) Schematic of power tower (b) virtual animation of power tower (c) heliostats based solar power plant, Japan [Segal et al., 1999]

Advantages

- Very high concentration ratio of 300 – 1500 can be achieved.
- Thermal energy storage is highly convenient with solar tower, thus rounding up for non – solar availability periods.
- They are quite large and thus get benefited from economic point of view.

- Power tower or heliostats scheme provides an excellently uncomplicated amalgamation with fossil powered hybrid engines.
- Very high temperature of operation allowing implementation of higher energy cycles.

Disadvantages

- Relatively expensive in contrast with parabolic trough collector.
- Complex structure as the receiver is located on the tower.
- Power tower or heliostats based power plants are generally very large *viz.* larger than 10 MW, to abridge the cost associated with such *'top notch'* technology.

.2.11 Heat transfer fluids (HTF)

Heat transfer fluid (HTF) is one of the most important constituent responsible for overall performance of the CSP. As huge quantity of HTF is required to be pumped through solar field to transport the generated heat, it is quite indispensible to minimize cost of HTF at the same time approaching for its high octane performance. With ferrying thermal energy from solar fields to power block, HTF can be easily used as thermal energy storage (TES) device, storing it into insulated TES tanks. Most suitable characteristics of the HTF includes thermal stability, high boiling point, very high thermal conductivity, low melting point, extraordinary specific heat capacity for energy storage purpose and low viscosity [Tina et al., 2013]. Broadly speaking, HTFs could be assorted into six groups namely:

- Air or other gases: Mostly are employed in non-concentrating technology.
- Water/steam: Utilised for direct steam generation (DSG) in PTC or LFR.
- Thermal oils: Employed in low temperature based LFR operation.
- Organics: Operated for low temperature PTC or LFR.
- Molten-salts: Best suited for high temperature power tower or heliostats.
- Liquid metals: Still under scientific developing stage.

Air is comparatively uncommon in large size solar thermal plants. Air can incorporate a wide range of temperatures and can be heated up to 700 ^{0}C at atmospheric pressure [Tina et al., 2013] and further can be used in steam production while exchanging its heat with water in some heat exchanger. The *'awe – inspiring'* advantage of air as a HTF is its cost – effectiveness and brilliant efficiency. Although, with a very good flow properties inside the transport pipelines (being due to very low kinematic viscosity), the major drawback of air as HTF is its corrosive nature due to oxidation at elevated temperatures [Feldhoff et al., 2014].

Main function of HTF is to convey heat from solar field to steam generator. If HTF is not water or steam, non – water based HTF whether it is thermal oil or some other organics would be used to carry the collected heat to the steam generator where working fluid which is water/steam would take the heat from HTF and passes this energy to the turbine to generate electricity. With HTF and working fluid both water (called direct steam generation (DSG)) complications are simplified many folds and the result is: improved cycle efficiency and decreased electricity cost. As a matter of fact, subjectively with the use of DSG, levelized cost of energy (LCOE) is reduced by 11% as compared to oil based HTFs and/or working fluids [Feldhoff et al., 2014].

Thermal oils have found their importance as HTFs in almost all around the world chiefly in PTC and LFR based power plants. Most primary of them includes synthetic oils, silicone oils and mineral oils. Thermal stabilities of these oils dwindle away at around 400 ^{0}C and that's the reason they are used for low temperature applications like LFR rather than PTC more preferably [Modi et al., 2014]. Thermal oils are extremely expensive and no literature is found regarding corrosion of metal – alloy piping.

Organics for example Biphenyl/Diphenyl oxide or TherminolVp-1 in common jargon is a big success in commercial CSP plants. It is also used in 1 MW PTC and LFR based CSP plant in Haryana, India under Ministry of New and Renewable Energy (MNRE) and National Institute of Solar Energy (NISE). TherminolVp-1 is a eutectic agglomeration of dual highly nonreactive compounds: Biphenyl ($C_{12}H_{10}$) and Diphenyl oxide ($C_{12}H_{100}$). With its working temperature range being very low, ranging around 10 – 390 ^{0}C [Tina et al., 2013].

Molten salts make an excellent HTFs due to most favourable thermal stability at elevated temperatures (above 1000 ^{0}C). Most importantly, at very high temperatures, molten salts show properties equivalent to that of water; for instance, vapour pressure and viscosity are closely akin. Molten salts are most pioneering technology used by *'state of the arts'* CSP plants based in France, United States and Spain, with Spain in its leading rein. In particular, an additional significant benefit of using molten salts as HTF in solar tower power (STP) is its ability for thermal energy storage (TES). As a matter of fact, a great many mainstream salts are centred on nitrates or nitrites such as $NaNO_3$ (60 wt. %) & KNO_3 (40 wt. %) [Tina et al. 2013].

Liquid metals have not yet latched any usage in concentrated solar power, though, they share very good thermo physical characteristics which makes them suitable for a HTF such characteristics include very high operating temperature range and thermal stability at elevated temperatures. Figure 2.12 gives an operating temperature range comparison between liquid metals and other *'state of the art'* HTFs. Investigations on liquid metals as a HTF are still on a

large.

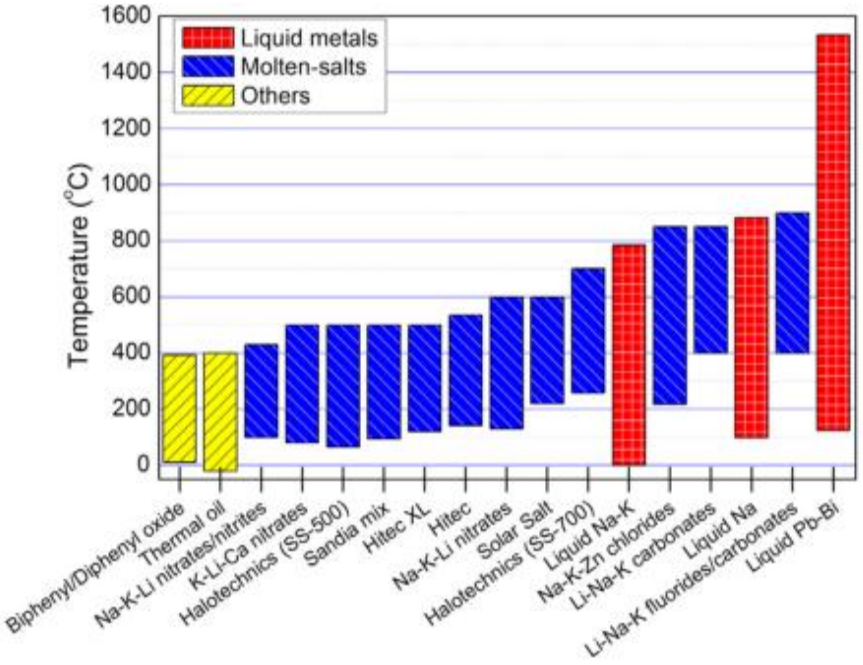

Figure 2.12 Working temperature range of different heat transfer fluids

[Vignarooban et al., 2015]

2.12 Thermal energy storage (TES)

Variable supply of solar energy for instance, weather influence and night hours gives a significant complications in utilizing the Sun's energy. Henceforth, an affordable and worthy thermal storage is extremely important for all year round working of the CSP plant. Two types of thermal storage are determined by intermittent and cyclic availability of solar energy namely short period and elongated period storage. While for the former case, spare energy which is harvested daily in the day period is stored for night usage, in the latter case, surplus energy gathered during summer and spring season is used to back up the low level of solar fluxes in winter season.

To illustrate, there are 3 methods which are involved for successful thermo – energy storage namely: Sensible heat energy storage, latent energy heat and chemical storage. For one thing, the former type of storage mechanism, features space heating a liquid or solid and isolating it from ambient while, waiting for its requirement to be used again. On the contrary, latent heat storage features phase change of storage material usually solid to liquid. More specifically, phase change induced latent heat storage accompanies a hefty amount of thermal energy storage at the same time maintaining constant temperature. Figure 2.13 illustrates

sensible and latent heat storage.

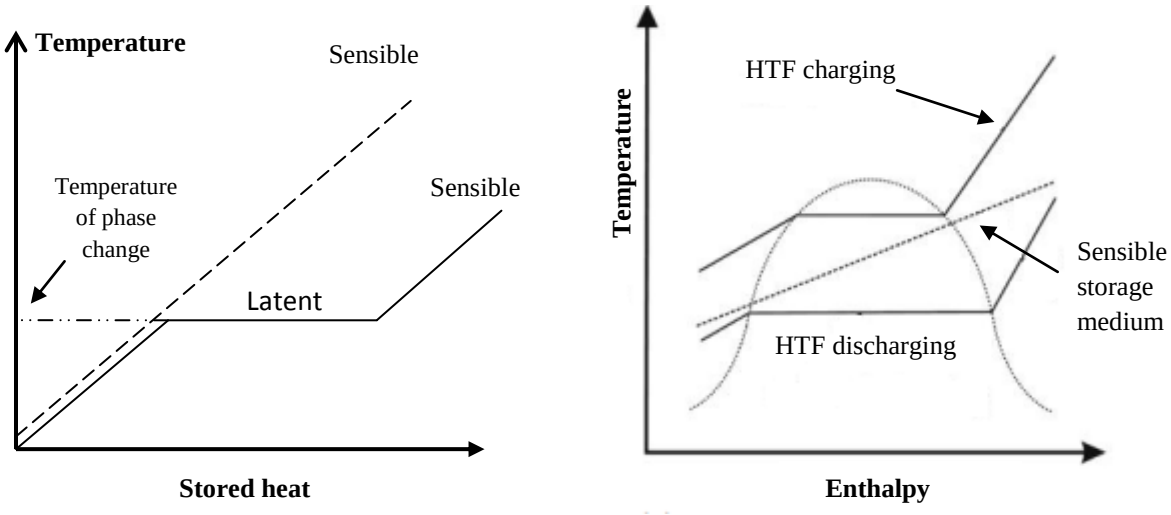

Figure 2.13 Sensible and latent heat storage mechanism of HTF [Vignarooban et al., 2015]

There are a lot of materials (solid or liquid materials) which can be suitably employed in sensible heat storage. For solid bed storage like solid NaCl, silica firebricks, reinforced concrete etc.; some sort of HTF is employed which circulates around the storage tank; takes thermo – physical exchange with solids and allow them to transfer heat by the method of convection. While on contrary, for liquid material heat storage, there is no requirement of any solid bed, it goes in a direct manner, *i.e.* HTF itself is responsible for heat storage, as it is directed and stored in insulating tank for a definite period of time.

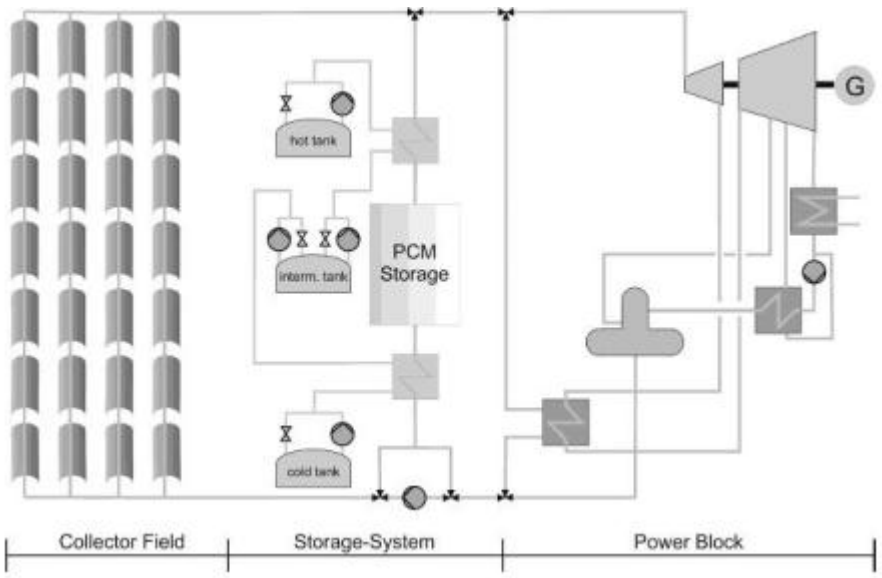

Figure 2.14 Methodology of CSP plant with thermal energy storage (TES) concept [Seitza et al., 2014]

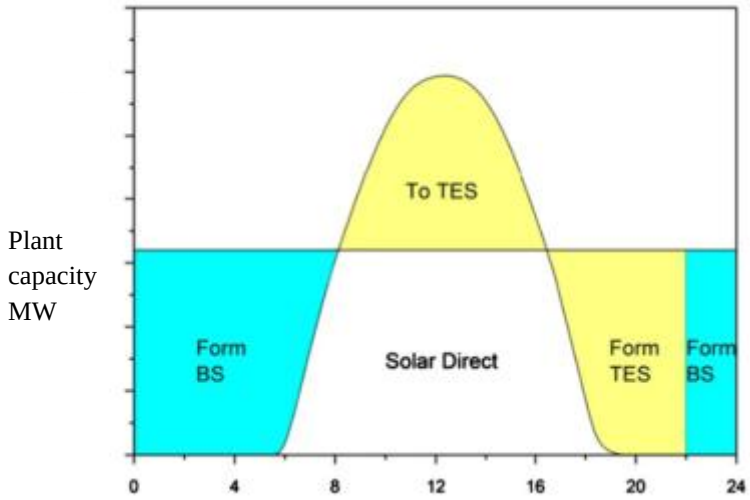

Figure 2.15 Power distribution using thermal energy storage (TES) and backup system (BS) [Vignarooban et al., 2015]

Yet another technology is chemical heat storage which employs harvesting heat energy in some kind of endothermic reactions which are reversible in nature and instituting for synthesis or de – synthesis. The energy used up in creating certain chemical product (ammonia, methane) could be deposited for indefinite period of time until it's the time of recovery where reverse exothermic dissociation reaction produces same amount of heat with little losses. Thus, chemical storage is best catch for extended duration storage purpose such as seasonal storage.

Figure 2.14 illustrates the working principle of CSP plant with TES consisting of one latent heat storage in form of phase change material, cold and hot insulated tanks for sensible heat storage [Seitza et al., 2014]. CSP efficacy could be boosted through consolidating two high end technologies which would also augment flexibility of the system. The duo conglomeration of (TES) and backup (BS) system both could be employed with CSP in order to maintain successful year round electricity generation. Backup system or more suitably fuel backup system assists to maintain constant generation particularly at peak periods. CSP backed up with backup system is called hybrid system. Backup system could be anything from fossil fuel powered to biogas powered or wind energy powered as well. Figure 9 shows the power distribution using TES and BS system.

2.13 Numerical model and estimation using ANSYS

Wang et al. (2015) studied and analysed the performance of parabolic trough collector under varying and inhomogeneous solar conditions utilizing finite volume method based numerical

approach of ANSYS FLUENT. Correspondingly, and as a matter of fact, solar ray tracing method was used to estimate and gauge the solar flux distribution and finally numerical methodology was used to gauge the influence of operating considerations on performance of absorber receiver system. It has been demonstrated by their results in numerical simulation that adverse circumferential temperature difference (CTD) decreased considerably with increase in velocity and temperature of HTF. Also, as the direct normal irradiance was increased a direct pattern of increment in CTD was observed. Maximum CTD approached in their simulation work was 105 K.

Tijani et al. (2014) simulated and demonstrated the radiation and convection losses related to the PTC receiver. Different parameters such as flow rate of Heat Transfer Fluid and wind speed were varied and their influence on convective and conduction thermal losses was explored. They came to the conclusion that the influence of wind velocity of about 3 m/s can increase the convection losses to about 64% while radiation losses being 36% of the total heat loss. Furthermore, their study found that convection losses are unswervingly influenced by the wind velocity in contrast to radiation losses from the glass envelope.

Al-Ansari et al. (2011) focused and studied convection and conduction losses of the air filled annulus PTC receiver system using numerical line of attack. The isothermal zones and streamline of the convection currents produced due to adverse circumferential temperature difference (CTD) of the absorber tube was graphically imitated and studied for the overall heat loss at varying CTD temperature of the absorber tube (refer fig. 2.16). It was concluded that overall losses are in direct proportion of CTD, in another words, peak hike worth of increment was noticed in overall heat losses as CTD was increased. Finally, they proposed an alternative as in the form of upper part insulation; where receives sparse concentrated radiation and concluded that as much as 25% reduction in total heat losses occurred in contrast to conventional receiver.

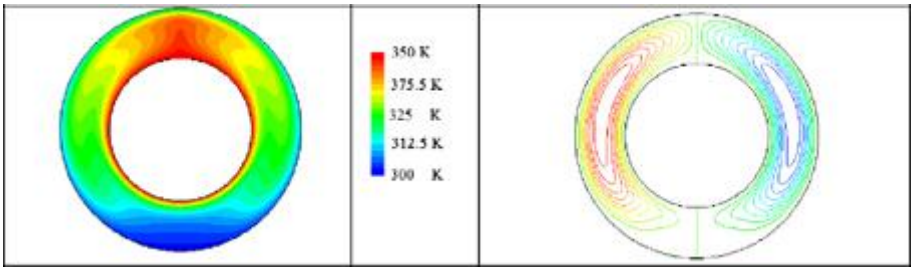

Figure 2.16 Isothermal zones and stream lines in air filled annulus [Al-Ansari et al., 2011]

Yaghoubi et al. (2013) studied and evaluated with the help of numerical simulation the influence and of fiasco in the receiver system subjected to lost evacuation in heat collecting tubes. 3 conditions of the receiver were studied namely: vacuumed, lost vacuum and broken tube and trio were numerically compared. After numerical and experimental validation, a conjecture was made regarding the heat losses in which they inferred that total heat loss due to lost vacuum amounts to not less than 40% which includes convective and radiation losses, as a result of this adverse increment of heat losses, thermal efficiency of collector was estimated to be reduced by 4 to 5%. In addition, estimates of broken tube suggested that 12 to 16 % of thermal efficiency degradation was corroborated in comparison of the previous case.

Alshahrani et al. (2005) studied convection in the cylinder annuli using numerical approach of finite element method conjugated with SIMPLER algorithm. Geometric values of the annulus chosen was D_o/D_i = 3, 4, 5. Convection currents, flow field or velocity vector and finally isothermal zones of the annulus were established for various operating parameters. Inferred results included the laminar condition of the flow field up to Rayleigh number of 10^5. Heat transfer phenomenon due to heated annulus was demonstrated with varying value of Nusselt number. Three heat zones were established namely: conduction heat zone where conduction was dominated for $Ra_m < 0.8$ and $k_e/k=1$; convection heat zone where convection was dominated for $Ra_m > 1.5$ and finally there was transition zone in between both of them.

Islam et al. (2012) envisioned and demonstrated in the absorber tube of evacuated receiver; the thermal features and characteristics with the help of 3-D simulation approach. FLUENT module of ANSYS was utilised for the development of computational model. Inferred that the hear flux around the absorber tube varied circumferentially on a piecemeal basis; which implies that lower part welcomes a good part of Sun's radiation, while, upper part was left frugal. Consequently, heat flux varied from as low as a few W/m^2 to 40 W/m^2 around the absorber tube. This circumferential temperature difference (CTD) was presented by the authors for different longitudinal geometric locations of 0.4 m, 4 m and 8 m which represented near inlet, in the middle and near outlet respectively. Finally, the authors calculated the circumferential temperature and concluded that it could vary in a typical industrial location from 560 to 650 K.

Egbo et al. (2014) emulated and simulated numerically the influence of annular gap on the efficacy and thermal performance of receiver system pertaining to parabolic trough collector. Annular gap ranging from 0.01 – 0.055 m was chosen by authors; whereas, they retained same

all rest of geometric conditions, design features of collector – receiver system, and metrological conditions. They concluded that as the annular gap between absorber and glass encloser was incremented; direct decrease in thermal performance of the receiver system was observed; henceforth, minimum gap range of around 0.01 – 0.040 m was prescribed by authors.

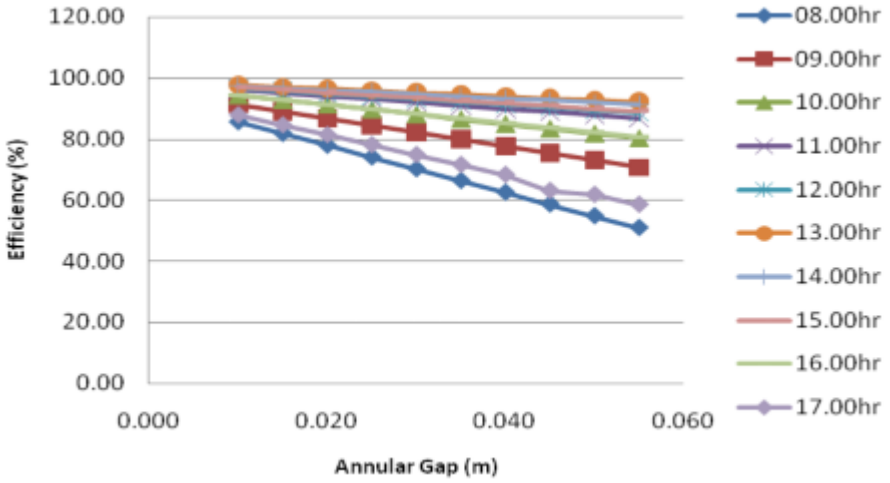

Figure 2.17 Influence of annular gap on thermal efficacy of receiver [Egbo et al., 2014]

Lobon et al. (2013) simulated receivers with direct steam generations (DSG) utilizing water as heat transfer fluid. Demonstrated graphically, the quality of steam at different longitudinal location and also for different circumferential temperature gradient; due to inhomogeneous solar influx conditions. Authors concluded that in DSG circumferential temperature gradient is influenced by the flow pattern of two phase flow of water – liquid mixture.

Zemler et al. (2013) numerically investigated the parabolic trough collector under the influence of wind forces. In their study, ANSYS CFx Module was explored to investigate two dimensional turbulent wind flow around the solar collector. In their study, authors linked direct relations of force or torque for different solar collector's alignment pertaining to different well documented wind velocities. Wind velocities ranging in 9 – 40 m/s were simulated and pressure contours were established for graphical study of pressure variations in the parabolic trough collector.

Jing – Lei et al. (2015) studied and investigated fluid flow, thermal stress and heat transfer in parabolic concentrator collector. For this purpose SRT method along with numerical approach was used to calculate the heat flux distribution around absorber. The main parameters which were changed are inlet velocity of the (HTF), direct normal irradiation (DNI) and the inlet

temperature of the HTF. The inlet velocity was varied in range 1 – 4 m/s, whereas, the DNI was varied from 500 W/m^2 to 1250 W/m^2. The inlet temperature of the HTF was ranged in 373 – 673 K. The investigated results includes: the solar flux distribution was not uniform in the circumferential direction. As DNI was increased, circumferential temperature difference (CTD) increased, whereas by the upsurge in temperature and velocity at inlet side of HTF, the CTD decreased. As inlet velocity of HTF is augmented, circumferential temperature gradient around the absorber tube was declined drastically, whereas HTF temperature difference kept on boosting by the rise in DNI. Stress distribution was also calculated, one end of the receiver was allowed to expand to see the thermal stress generated in it. Finally, the glass cover expand less as compared to the receiver tube, the expansion was mainly in the Z – direction. The results were validated by simulation done by solar ray trace method (SRT).

Marif et al. (2014) studied and simulated the thermal performance of two receivers based on water and synthetic oil called TherminolVp-1^{TM}. For mass flow rate and inlet temperature of 0.2 kg/s at 25 ^{0}C respectively, both the PTC receivers were simulated for the turbulent flow and their comparative thermal performance was evaluated by the authors. It was further reported that convective heat gain from absorber tube to HTF is directly dependent on the thermo – physical characteristics of HTF. For the stated reason, that due to lower value of dynamic viscosity and comparative higher value of heat conductivity, mean wall temperature of absorber was high for the case of synthetic fluid, this resulted in escalated glass envelop temperature and hence elevated radiation and convection losses. Henceforth, with synthetic oil as HTF, overall thermal efficiency was reduced by 3% as compared with water as HTF. Finally, author suggested that water is best suited for improved thermal performances in PTC power plants related to lower temperature ranges.

He et al. (2010) heat exchange mechanism in PTC receiver/absorber system was numerically studied by authors using Monte Carlo ray tracing scheme and finite volume method. At first, solar irradiance over the receiver was simulated using MCRT technique and was further validated with the heat flux distribution of absorber. This validated result was utilised to simulate the complex heat transfer and fluid model of receiver system. Authors concluded that heat flux distribution is highly dependent on the geometric parameters like geometric concentration ratio and rim angle. Also, with increases in geometric concentration ratio, the heat flux distribution became more dispersed, with increase in rim angle the maximum and minimum value heat flux was decreased thus giving a favourable temperature gradient on the receiver system.

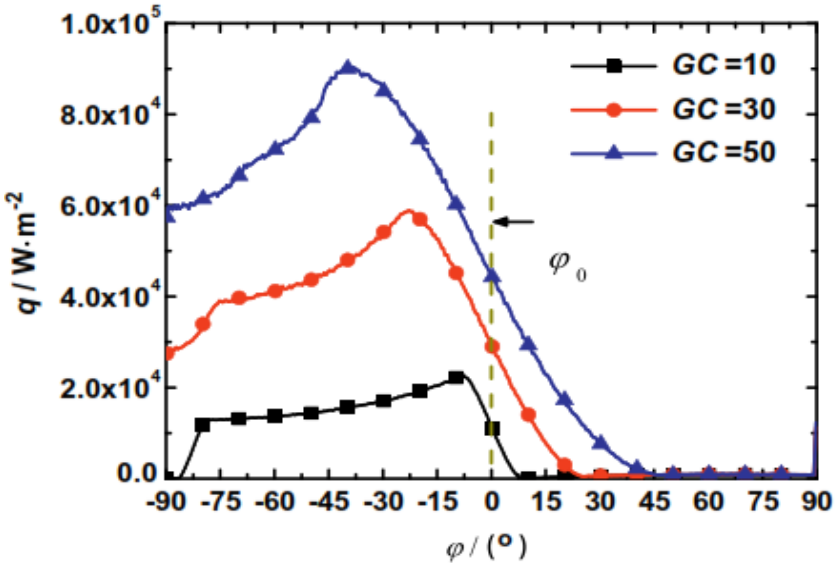

Figure 2.18 Variation of heat flux with different geometric concentration ratio [Ya-Ling et al., 2010]

Cheng et al. (2010) simulated and modelled the adverse heat flux distribution on the absorber tube by employing Monte Carlo ray tracing technique. Coupled heat transfer phenomenon was numerically simulated using MCRT coupled with ANSYS FLUENT. Numerical simulation results were demonstrated graphically, which predicted the influence of direct normal irradiance (DNI), emissivity of inner tube wall and Reynolds number on outlet temperature, absorber outer wall temperature and thermal radiation losses respectively. Thermal losses decreased with increase in R_e and amplified with I_b and ε_w. With rise in R_e thermal losses declined due to the fact that with escalation in R_e flow rate was augmented and hence loftier heat absorption capabilities. While, with surge in I_b the absorber temperature enlarged but keept the flow rate constant resulting in decline in heat absorption capabilities of HTF, this escalated the T_w (wall temperature) hence radiation losses proliferated. Finally, with higher ε_w larger radiation thermal losses resulted.

Paetzold et al. (2014) performed numerical approach to minimise the thermal losses and wind load on the solar collector, it was investigated that air flow on receiver tube of solar collector have high impact on overall efficiency of the parabolic trough power plant. It was found by the investigation that larger the thin structure of the collector larger would be aerodynamic forces. The pitch angle was varied, and bring into being that if it was greater than 15^0 and smaller than 60^0, structure felt high aerodynamic forces. Same result was established that by increasing the focal length of trough, pitch moment was also amplified with escalation in depth of trough. It was established; deeper the trough, higher the sheltering effect which

caused the thermal losses to be reduced due to forced convection. The results were validated the three dimensional simulation by the commercial CFD program ANSYS CFX 14.5.

2.14 Thermal model and performance of PTC

Lufpert et al. (2010) studied and evaluated experimentally, overall thermal properties of parabolic trough collector and their influence on the efficacy of PTC system. Authors developed peculiar methods to calculate heat losses in receivers by taking into considerations the energy balance equations driving the heat mechanism from hot walls of inside tube receivers up to the surrounding. Authors experimentally calculated and finally modelled the relation between glass outer wall temperature and the convective heat transfer losses from outside glass envelop. '*Awe – Inspiring'* findings in the work was their conclusions on the overall thermal losses on a typical solar power plant based on PTC operating under 390 ^{0}C of temperature, which was around 300 W/m. Equation given below was modelled by the authors to calculate the convective thermal losses of receiver, where Nu is Nusselt number for forced convection conditions of wind flow.

$$Q_{g-conv} = \pi \Delta l \lambda_g Nu_{g-a}(t_g - t_a) \tag{2.1}$$

Mullick et al. (1989) a better – quality and upgraded strategy was adopted by the authors to calculate the overall heat loss in an archetypal hollow tube shaped absorber typically targeted for PTC practice. This method beautifully predicted the overall heat loss of the absorber operating within the range of 60 – 270 ^{0}C with wind velocity ranging between 2 – 10 m/s and absorber diameter between 15 – 75 mm. Though this method could also be used for absorber systems working under temperature of 350 ^{0}C, however, maximum of computational error thus observed could be within 4% of the iterative solution errors. The relation thus developed left no specific convective heat transfer (h_w) dependency of the absorber system and nicely and smoothly predicted the overall heat loss factor simply depending on wind velocity. Following equation predicts the heat convection factor for the convective loss around any typical absorber.

$$h_w = 4V_w^{0.58} D_2^{-0.42} \tag{2.2}$$

Padilla et al. (2014) studied and presented exergy analysis of PTC in order to study the influence of ambient or surrounding to the heat transfer mechanism of receiver system. The chief components under investigation were solar irradiance, mass flow rate of HTF, inlet temperature of heat transfer fluid, wind speed and pressure in annulus. It was concluded that if the pressure in annulus was below 1 torr convective heat loss was relatively insignificant inside the annulus. However, if this pressure was increased greater than 1 torr, convection heat losses were significantly escalated hence contributing towards exergy destruction. Authors concluded that receiver's performance was gravely dependent on the vacuum inside annulus. If vacuum is maintained inside annulus, even convective losses from glass envelop could be subdued easily. This fact is further corroborated by the fig. 2.19.

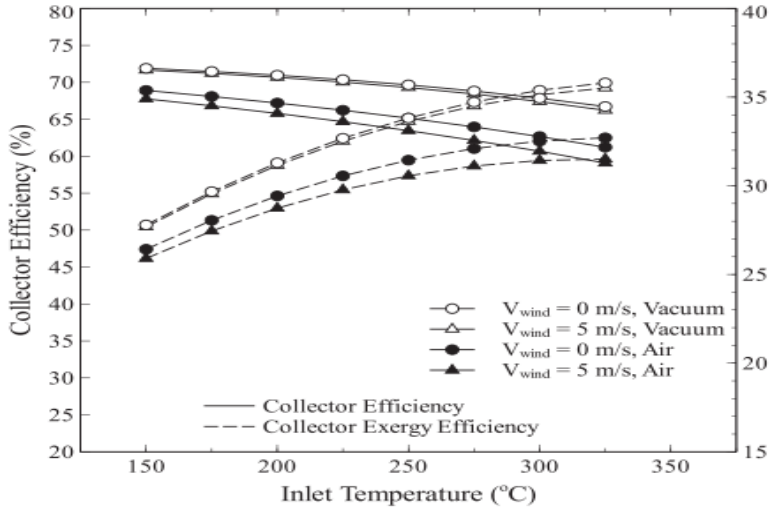

Figure 2.19 Exergy analysis and convective loss dependency of vacuum in annulus

[Padiala et al., 2014]

Liang et al. (2014) studied and compared analytically diverse thermal models pertaining to the solar parabolic trough collector system. Evaluation of all the heat transfer procedures were progressed in the receiver/absorber this included convection heat transfer from absorber to HTF, from absorber to glass tube, from glass tube to surrounding. Conduction heat transfer from absorber to glass tube, from absorber to support brackets and from glass cover to absorber as well and finally radiation heat transfer from glass cover to ambient, from absorber to glass cover etc. Analytically evaluated the model that may be used to calculate the convection heat loss from the absorber to glass tube for varying pressure in the annulus and for vacuum and finally modelled a mathematical equation for the same. Equation 2.2 gives the relation to calculate convective coefficient for pressure higher than 0.013 Pa in the annulus

$$h_{a-g} = \frac{2\lambda_{eff}}{d_{r-o} \ln(d_{g-i} / d_{r-o})} \tag{2.3}$$

Seitze et al. (2014) studied and proposed different storage concepts for direct steam generation solar power plants (DSG). One technical glitch with using superheated steam was that its specific heat kept changing with temperature, while, storage medium based on molten salts has a constant specific heat. Henceforth, the use of ordinary heat exchangers resulted in inefficient heat transfer process by reducing the favourable live steam temperature which ultimately and eventually reduced the power block efficiency. Method proposed to eliminate the aforementioned glitch was: the usage of three tanks for the storage of sensible heat i.e. cold tank, hot tank and intermediate tank. Correspondingly, higher mass flow rate would be used for cold tank and vice versa for hot tank would be operated. With this, temperature profile of both Steam and HTF would be in complete congruence at each step and better heat transfer coefficient could be maintained for efficient latent and sensible heat storage. Figure 2.20 shows the arrangement of trio heat exchangers, hot tank has a lower mass flow rate corresponding to the higher steam temperature at state 1, while, intermediate tank and cold tank has subsequent higher mas flow rates.

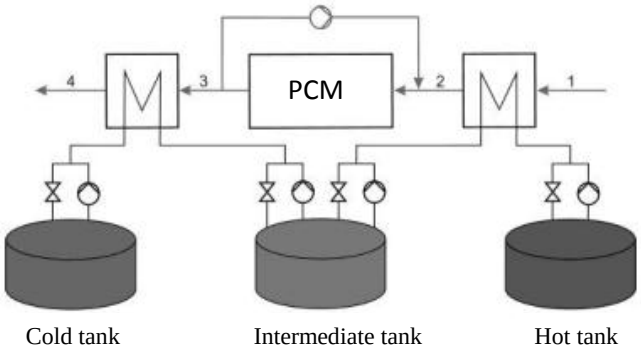

Figure 2.20 Improved DSG storage concepts [Seitze et al., 2014]

Gharbi et al. (2011) studied and presented comparative illustrations in the parabolic trough collectors (PTC) and linear fresnel collector (LFR). Performance of both PTC and LFR was numerically studied .The influence of ambient temperature, solar irradiance, and mass flow rate was studied. The efficiency of PTC collector was discussed which was dependent on operating temperature of collector, direct normal irradiance, and the incidence angle of solar irradiance. The efficiency was defined as the ratio of total heat transferred in HTF to direct normal irradiance on aperture eq. (2.5). While heat transferred to HTF (Q_c) is defined as by

eq. (2.7). Where A_c is aperture area, U_c is heat loss coefficient which is a direct function of temperature difference between absorber and ambient, η_o is the optical efficiency which depends only on the mirror parameters like reflectance, absorptance, transmittance, mirror intercept factor and angle of incidence.

$$\eta = \frac{Q_u}{I_b . A_c} \tag{2.7}$$

$$Q_u = \eta_o I_b A_c - U_c (T_c - T_a) A_a \tag{2.8}$$

Kun-wang et al. (2015) studied and calculated the relation between the focal length of the PTC and the figurative characteristics of the collector system of PTC. The effect of defocusing phenomenon and design parameter was taken into consideration on yet wide-ranging features and the efficacy of complete working of photo thermal conversion was numerically studied. Studies in parameter relations were done by the different possible combination of the aperture width, focal length and finally focal length to aperture width ratio. This was done by having 'f' constant and 'a' varying, having 'a' constant and 'f' varying, and hence four cases were taken into consideration. The rim angle and the concentration ratio was also taken into consideration, and it was found that the concentration ratio was proportional to 'a'. The solar heat flux increased with surge in 'a', but it did not went in the same manner, it decreased after a particular value of 'a'. Same trend was found for the wall temperature distribution. The thermal efficiency always monotonically improved with 'a'. The optical efficiency of the trough first amplified with 'a' up to a maximum value of 71.19% , than it went on declining greatly with further rise in 'a'.

CHAPTER 3

EXPERIMENTAL WORK

The main objectives of this chapter are to provide the details of test facility, instrumentation and operational procedures. Experiments were performed for wide range of air velocity, mass flow rate of HTF, inlet temperature of HTF, direct normal irradiance (DNI). Finally numerical simulation methodology of FLUENT code of ANSYS is utilised to evaluate the heat loss patterns in the industrial receiver with well documented cases of industrial thermo physical parameters. Lastly, a profitable alternative is proposed to curb those adverse losses and both are compared graphically.

3.1 System description

A grid – connected solar thermal power plant, with a gross capacity of 1 MW at direct normal irradiance (DNI) of 600 W/m^2, has been designed and commissioned in the campus of National Institute of Solar Energy (NISE) at Gwal – Pahari near Gurgaon by IIT Bombay as a part of the project entitled *'Development of a Megawatt – scale Solar Thermal Power Testing, Simulation and Research Facility'*. The unique feature of the plant is the integration of two different solar fields (parabolic trough collectors and linear fresnel reflectors) without a fossil fuel backup. The plant combines the advantages of synthetic oil based parabolic trough collector (PTC) field and direct steam generation (DSG) of linear fresnel reflector (LFR) field. The heat supplied for generation of steam is received from two different solar fields. The Parabolic trough collector (PTC) field (aperture area of 8175 m^2) supplies about 60% (3 MW) of the required heat, while, the linear fresnel reflector (LFR) field (aperture area of 7020 m^2) supplies the balance about 40% (2 MW) of the required heat at design condition.

The PTC field uses concentrated solar radiation incident on it to generate high temperature oil at 390 ^{0}C, which is fed into the heat exchanger. Simultaneously, the LFR field generates saturated steam at 44 bars and 256 ^{0}C which is added to the steam generator. At the outlet of the LFR field a two-phase mixture is obtained. The mixture enters a drum, where the saturated steam is sent to the heat exchanger and the liquid is re-circulated to the LFR field inlet. HTF is used for both steam generation and superheating.

Figure 3.1 Test facility of 1 MW CSP plant employing PTC and LFR solar fields, [NISE, India]

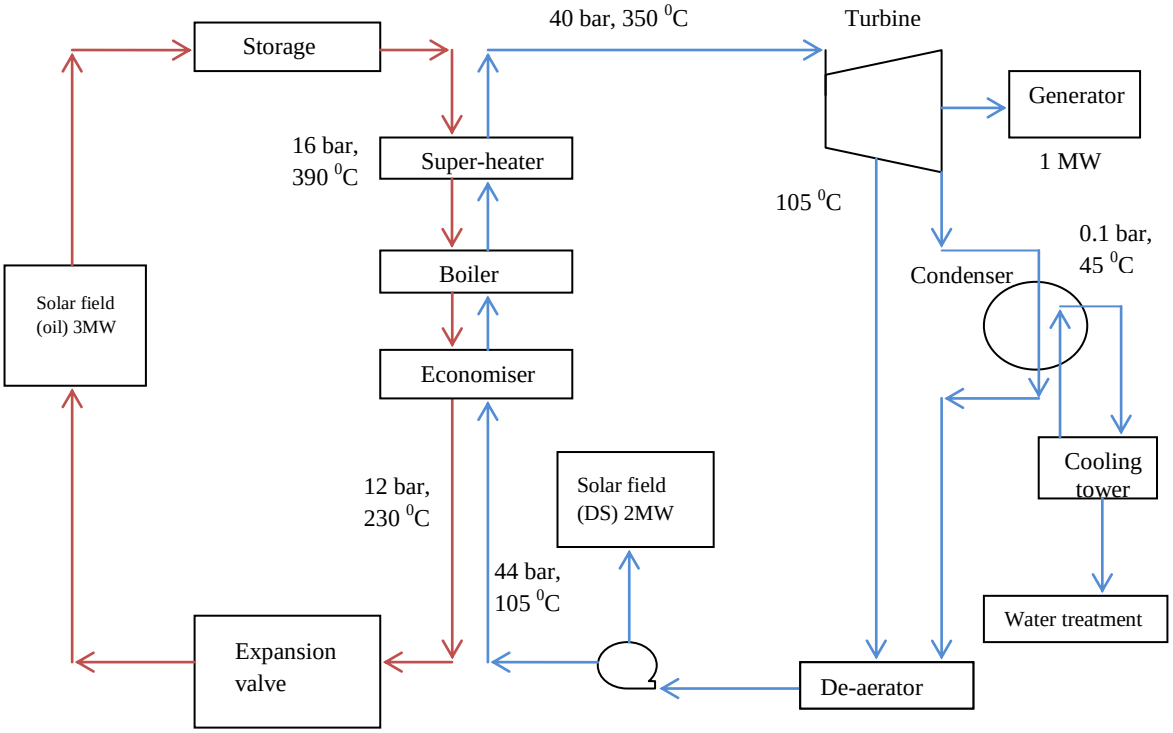

Figure 3.2 Schematic of test facility

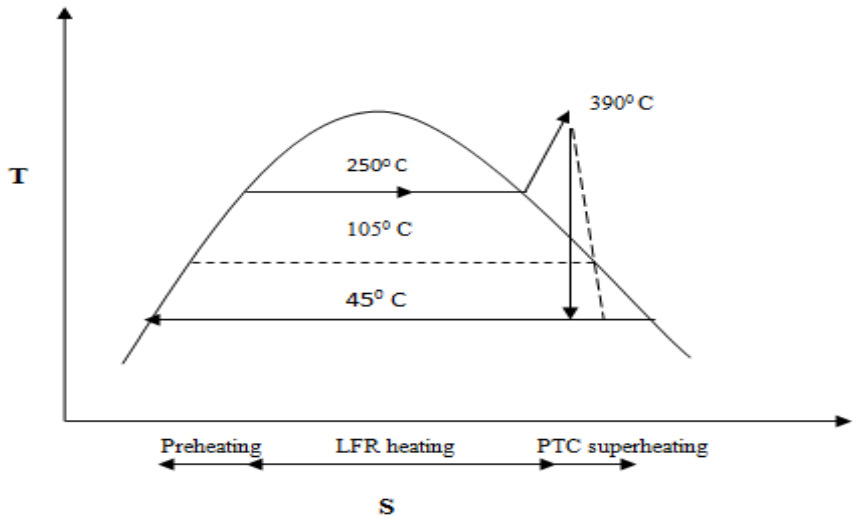

Figure 3.3 Temperature *vs.* entropy diagram of the CSP plant

The steam mass flow rate, pressure and temperature at the inlet of the turbine are 1.93 kg/s, 40 bars and 350 ^{0}C respectively. The plant works when reasonable quantity of solar radiation is available and uses a small amount of thermal energy storage (for about 20 min) as transient back – up.

This experimental arrangement is a whopping, "8175 m^2 parabolic trough collector (PTC) based, 1MW concentrated solar power plant," commissioned in, Gurgaon city, Haryana, India. The distinctive parameters of the establishment are shown in Table 3.1. Figure 3.2 describes the schematic of trio – looped, parabolic trough collectors, working on oil as HTF is hooked up with water based LFR fields. TherminolVp-1 is used as heat transfer fluid (HTF) in PTC fields, which is water white liquid of very low viscosity composed of Biphenyl/Diphenyl Oxide (DPO) eutectic mixture. TherminolVp-1 peculiarly, does not decompose within its working range of 327 – 768 K; which is the most favourable temperature range for current experimental establishment.

Figure 3.3 demonstrates the temperature entropy diagram of the power block working on Rankine cycle. It is ostensibly explicit that the water coming into LFR fields is preheated in shell and tube type economiser working in the operating conditions given in Table 3.1. While, water is converted into saturated steam in Linear Fresnel (LF) fields which produces steam at 250 ^{0}C and 45 bars in steam generator whose operating parameters are given in Table 3.2. Finally this saturated steam is superheated in super heater; which is actually a multiple pass shell and tube heat exchanger working under operating conditions given in Table 3.3 with the help of TherminolVp-1 oil coming from parabolic trough fields operating at 390 ^{0}C and 40

bars. This superheated steam is than expended in a multistage condensation turbine powered with Rankine cycle.

Table 3.1: Operational parameters of economizer

	Shell	Tube
Operating Pressure (bar)	14.5	45
Operating temperature (IN/OUT) (^{0}C)	264/231	105/232

Table 3.2: Operational parameters of steam generator

	Shell	Tube
Operating pressure (bar)	44	15.1
Operating temperature IN/OUT (^{0}C)	232/256	364/264

Table 3.3: Operational parameters of super heater

	Shell	Tube
Operating pressure (bar)	16.5	43.5
Operating temperature IN/OUT (^{0}C)	390/364	256/350

3.2 Components and system specification

System specification includes the general specifications of the concentrated solar thermal power plant's operational equipment's and components. Table 3.4 illustratively demonstrates the wide spectrum system specification in a glance.

Table 3.4: System specification at a glance

S. No.	**Components**	
1.	**System Unit**	**Specification**
	Parabolic Trough Collector (PTC)	
	Length of single trough	12.5 m
	Width of single trough	5.57 m

	No. of troughs in one row	20
	No. of rows	6 parallel rows (3 loops)
	Length of each row	250 m
	Aperture of single trough	136.25 m^2
	Total aperture of parabolic trough	8175 m^2
	Material	Stainless steel
	Tracking	Double axis tracking
	Concentration ratio	85
	Rim angle of each trough	70^0
	Heat transfer fluid (HTF)	TherminolVp-1
	Recirculating Pump capacity	15 kW
	Operating temperature	390 ^{0}C
	Operating Pressure	40 bar
2.	**Compact Linear Fresnel Reflector (CLFR)**	
	Total aperture of Fresnel reflector	7020 m^2
	Length of each row	240 m
	No. of rows	2 parallel rows
	Heat transfer fluid (HTF)	Water as direct steam generation (DSG)
	Recirculating pump capacity	18.5 kW
	Operating temperature	257 ^{0}C
	Operating pressure	45 bar
3.	**Receiver/Absorber**	
	Length of each absorber	12.5 m
	Outer dia. of glass envelop	0.1205 m
	Inner dia. of glass envelop	0.1115 m
	Outer dia. of absorber	0.0720 m
	Inner dia. of absorber	0.0705 m

	Absorber glass	Silicate glass
	Absorber Steel	321-H stainless steel
	Absorptivity of absorber tube	0.95
	Emissivity of absorber tube	0.12
4.	**Power Block (Turbine)**	
	Turbine	Condensation turbine
	No. of stages	5 stages
	Operating pressure	40 bar
	Operating temperature	350 ^{0}C
	RPM	8167
5.	**HTF Storage Unit**	
	High temperature capacity	18 m^3
	Low temperature capacity	16 m^3
	Material	SS
	Insulation	Glass wool
	Working fluid	TherminolVp-1
6.	**Alternator**	
	Power rating	1500 kVA
	Voltage	415 Volts
	Current	208.8 amps
	Power factor	0.8

3.4 Operational procedure

A touchstone operational procedure soundly associated with previous research work was adopted for the sake of standardisation of results that could be compared and paralleled with the well documented cases of foregoing research. Experiment was performed for redundant and copious values of thermo physical parameters which directly influence the efficacy of

PTC receiver system. As a matter of fact, this redundancy in experiment was done due to the fact of reproducibility of the results. For instance, these thermo physical properties includes direct normal irradiance (DNI), mass flow rate of heat transfer fluid (HTF) , inlet and outlet temperature of HTF and wind velocity. Mostly, the varied thermo physical parameters were controlled *via.* data logger using SCADA system. However, their effect on the PTC receiver system was estimated by pre – calibrated sensors. These sensors include, resistance temperature detector (RTD) for temperature sensing at various locations such as inlet and outlet of each parabolic trough, mean surface temperature of absorber and glass enclose etc. The solar intensity or direct normal irradiance, wind velocity and ambient temperature are measured in Weather station of NISE by using equipment's such as industrial Pyronometer and Anemometer. Round trip data is recorded and managed using data logger in SCADA software and on the basis of recorded data, efficacy in the form of thermal efficiency of the PTC receiver system was calculated with varying dominant parameters. Finally, on the basis of industrial data related to PTC receiver thus generated, was used to simulate the circumferential temperature difference (CTD) and heat loss mechanism in the conventional air filled receiver and an comparative analysis with the new proposed one side insulated is suggested. For the simulation purpose, FLUENT module of ANSYS was utilised and its numerical methodology was necessitated.

The standard procedure of experimentation is enlisted as follows:

a. Firstly, two ways tracking device of the parabolic solar fields was turned on, in order to face and track the continuous moment of sun. This ideal tracking was done for approximately 30 minutes until the mean temperature of absorber wall was reached around 350 ^{0}C
b. After 30 minutes of continuous ideal tracking of solar fields, PTC recirculating pump was turned on and fluid was made to circulate in the receiver. Pump is a recirculating type having a capacity of 15 kW.
c. Readings were withheld until 60 minutes of its operation to make plant under steady running conditions.
d. For the calibration purpose, mass flow rate of heat transfer fluid (HTF) was held constant for almost 30 minutes and the net temperature rise in heat transfer fluid (HTF) was observed relative to time. An undeviating rectilinear relation suggests all the temperatures sensors are perfectly working.
e. The system was started at 9:00 O'clock in morning and readings were recorded every minute using data logger powered SCADA software.

f. Experimental readings were taken for thermal efficiency, glass envelope temperature, outlet temperature and absorber temperature as a consequence of varying mass flow rate, and wind velocity.

g. The experiment was repeated every day from 9 O' clock in morning till 3 O' clock in afternoon for the sake of reproducibility of the results.

h. Finally, the receiver data was used in ANSYS simulation to calculate the circumferential temperature difference (CTD) or circumferential temperature gradient in the absorber of conventional air filled annulus receiver and was graphically compared with new improved one side insulated receiver.

i. In addition, overall losses and convective losses due to wind velocity were also graphically compared with the new improved receiver utilizing FLUENT module of ANSYS 15.0 version.

CHAPTER 4

EXPERIMENTAL FINDINGS

The following results were gathered and are represented below graphically.

4.1 Variation of thermal efficiency of collector with mass flow rate for different inlet temperature

Thermal efficiency is defined as the ratio of thermal heat absorbed (Q_u) by heat transfer fluid (HTF) to the direct normal irradiance on the collector aperture.

$$\eta = \frac{Q_U}{I_b . A_c} \tag{4.1}$$

Where,

Q_u = Total heat gained by heat transfer fluid (TherminolVp-1) = $m.C_p.\Delta T$

I_b = Direct normal Irradiance (DNI). Cosφ

A_c = Aperture of collector.

It is ostensibly explicit that thermal efficiency of the collector has increased as the mass flow rate of heat transfer fluid (HTF) was augmented upto a certain limit i.e. from 0.2 kg/s to 1 kg/s. However, if mass flow rate was further up surged after this limit, there was no appreciable growth in thermal efficiency was perceived, rather saturation was observed. This is further corroborated by the fig. 4.1 in which if mass flow rate is increased further up to 1.8; for all the inlet temperatures, thermal efficiency is almost uninfluenced regardless of inlet temperature and mass flow rate.

In addition, fig. 4.1 also infers the influence of inlet temperature of heat transfer fluid (HTF) on thermal efficiency of collector. It is clear that as the inlet temperature is increased thermal efficiency drops for all the values of mass flow rate. The possible reason for this might: with the increase in inlet temperature heat capacity of the HTF is reduced and henceforth maintaining a lower inlet temperature for all mass flow rates might be beneficial for high octane performance of collector. Furthermore, maximum thermal efficiency reached was 43.5% for the corresponding mass flow rate and inlet temperature of 1 kg/s and 180 ^{0}C. To take maximum utilization of HTF per cycle, it is necessary to decrease the temperature of HTF at inlet to a minimum approachable value and this is done by the economiser, where

temperature of HTF is reduced to increase the temperature of feed water to the boiler.

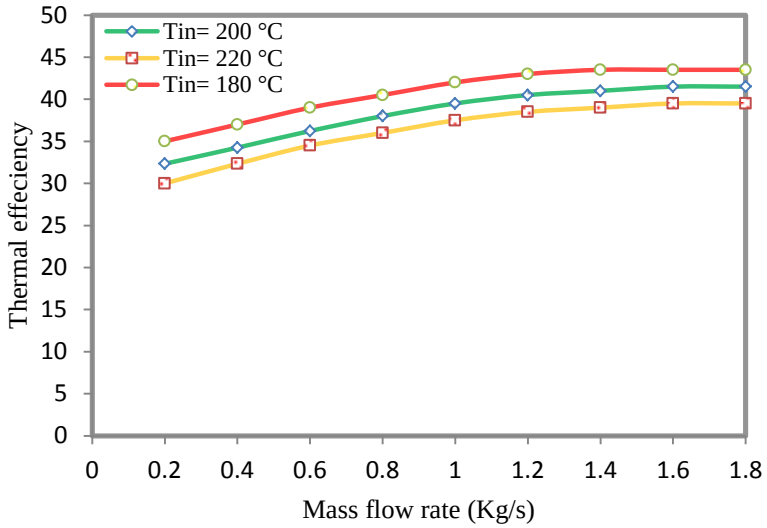

Figure 4.1 Variation of thermal efficiency with mass flow rate at different inlet temperature

4.2 Variation of glass envelope temperature, mean absorber temperature and outlet temperature with respect to mass flow rate of heat transfer fluid (HTF)

The influence of mass flow rate of HTF on the absorber tube temperature, glass tube temperature and outlet temperature of HTF was studied and illustrated in the fig. 4.2. To begin with, outlet temperature and absorber temperature was found to be inversely proportional to mass flow rate, being to their lowest value against 1.2 kg/s. As mass flow rate was further reduced, considerably from 1.2 kg/s to 0.6 kg/s, noticeable increase in both temperature took place. For instance, when mass flow rate was 0.8 kg/s the outlet temperature was approximately 395 ^{0}C, while, mean absorber temperature and glass tube envelope temperature were 390 ^{0}C and 370 ^{0}C respectively. To explain, as the mass flow rate was amplified, more mass flow of HTF is circulated for the same amount of heat flux around absorber, thus taking more heat from it and cooling it down more uniformly, henceforth, the cause is surge in mass flow rate of HTF while, the effect is decline in absorber temperature. Furthermore, as absorber temperature is diminished with escalation in mass flow rate of HTF, glass envelope temperature is also reduced piecemeal due to the fact that with the reduced temperature of absorber entails as a logical consequence of less radiation heat transfer into the glass envelop according to Stephan Boltzmann law.

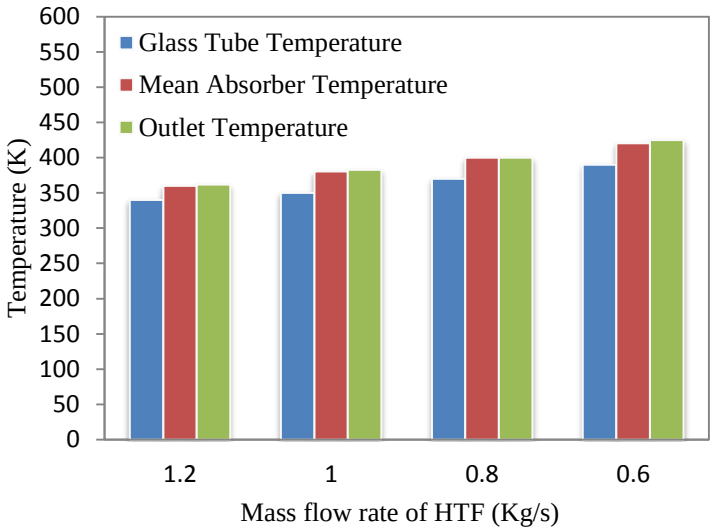

Figure 4.2 Temperature variations with mass flow rate of HTF

4.3 Variation of glass envelope temperature with respect to wind velocity

Glass tube temperature has a direct consequence on convection losses by natural convection from envelope. The reduction in glass tube temperature with wind velocity connotes escalation in convection losses across the glass tube. Figure 4.3 demonstrates the direct influence of wind velocity over the glass tube temperature. To illustrates, in the experiment wind velocity was measured and was plotted in range of 0.6 – 5 m/s which is according to the weather conditions and complying with the previous research documented cases. It is explicit from the following figure that as the wind speed was increased from 1 m/s to 4 m/s, considerable drop in glass tube temperature was witnessed for practically all the values of mass flow rate. This diminution in glass tube temperature was reported due to the reason of escalation in convection losses with rise in wind velocity. In another words, due to upsurge in value of coefficient of convective heat transfer with wind velocity, glass tube temperature was reduced substantially. This fact is further corroborated by Table 4.1 in which wind velocity is measured in the range of 1 – 4 m/s and its corresponding calculated value of convective heat transfer coefficient is given for the mass flow rate of 1.2 kg/s and 0.8 kg/s. To quantify, Table 4.1 depicts the wind velocity in range of 1 – 4 m/s which is actually the common documented case of wind flow in the month of September. Furthermore, wind flow rate is accompanied by its respective coefficient of convective heat transfer which was calculated by correlation deduced by Mullick et al., [1986]. It can be easily perceived that as wind velocity is increased, coefficient of convective heat transfer is also increased almost linearly, being maximum 19.45 W/m^2 K for wind velocity of 4 m/s and corresponding glass tube temperatures for mass flow rate of 1.2 kg/s and 0.8 m/s are 334.93 K and 342 K respectively.

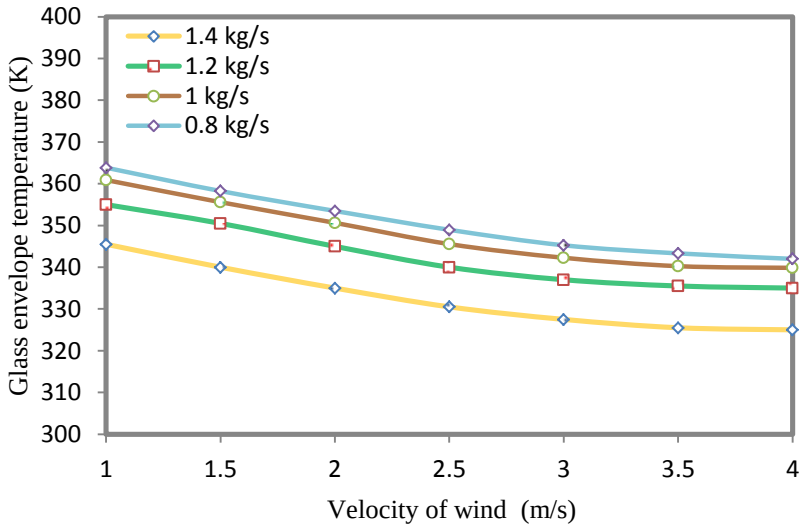

Figure 4.3 Influence of wind velocity on glass envelope temperature.

Table 4.1: Wind velocity with its convective heat transfer coefficient and glass tube temperature

Velocity of wind (m/s)	Convective heat transfer coefficient (W/m^2k)	Glass tube temperature (K) with mass flow rate of 1.2 kg/s	Glass tube temperature (K) with mass flow rate of 0.8 kg/s
1	9.72	355.8	363.84
1.5	11.9	350.48	358.25
2	13.75	344.89	353.48
2.5	15.38	340.83	348.96
3	16.85	336.78	345.25
3.5	18.20	335.21	343.31
4	19.45	334.93	342

CHAPTER 5

NUMERICAL METHODOLOGY USING ANSYS SIMULATION

This section deals with the simulation of conventional air filled receiver experimented with, at National Institute of Solar Energy (NISE), Gurgaon, Haryana. The drawbacks of the conventional receiver would be brought to attention and would be figuratively and graphically compared with the new '*avant – grade',* proposed one side insulated receiver. Meanwhile, two subtle glitches regarding subpar performance of conventional air filled receiver is demonstrated in the overleaf paragraph which would serve as underpin for the upcoming evaluation. In later sections of this chapter, physical model of the new insulted receiver would be described with the help of geometric model of heat exchange scheme, ANSYS model with governing equations and numerical model with meshed geometry.

To begin with, high octane performance of solar fields or collectors is undeniably indispensable for parabolic trough technology. A decade long of research on parabolic trough technology has been summed up by Fletcher [2001] and David et al. [2011] who clearly adduced the work of Steinmann et al. [2005]; Arasu et al. [2005]; Dudley et al. [1994]; Alguacil et al. [2013]; Zhang et al. [2014]. These interesting and invaluable research includes—but, are not limited to: (1) performance and analysis of heat transfer fluids and thermal storage, (2) support structure and reflector development, (3) receiver development, (4) process development for direct steam generation, (5) numerical optimization of thermal physical factors. In addition, Thermo physical parameters such as solar irradiance, wind velocity and mass flow rate; and inlet temperature of heat transfer fluid (HTF) are urgently critical, in order for parabolic trough collector (PTC) to vie for perfection in performance. To illustrate, at present, vacuum filled annulus is being used as a *'nouveau technology'* to put down any natural convective losses, (fig. 5.1(a)). Nonetheless, they are high-priced and may entail adequate up to 20% cost of the solar PTC field [Sargent et al., 2003]. Which is way too much high as far as overall cost of the PTC based concentrated power plant is considered.

Furthermore, for the purpose of lower temperature applications such as process heat and water heating, less expensive air filled annuli receivers are presently used. A good deal of

work on industrial process heat application and heating & cooling is presented by Sozen et al. [2002] and El Fadar et al. [2009]. These receivers owing to lower thermal efficiency at higher temperatures; due to convection currents are not used for power production. These Buoyancy prompted convection currents are resulted from temperature difference of absorber and the glass tube. Figure 5.1(a), fig. 5.1(b) and fig. 5.1(c) demonstrates the typical velocity vectors, streamlines function and isothermal zones of a typical air-filled annulus receiver with an aspect ratio $D_0/D_i = 4$. Such buoyancy induced natural convection currents are in perfect qualitative agreement of Kuehn et al. [1974] and Liu et al. [1961]. That is to say, two primary eddies are developed due to the buoyancy impelled flow in the near vicinage of hot and cold walls of the receiver. As a matter of fact, convection currents instigated by temperature difference of absorber and glass tube for, not less than de facto 35% of total convection losses in a PTC receiver system [Alshaharani et al., 2015]; which appears to be a sombre issue that must be put attention to. Moreover, design of the conventional air filled annulus receiver, lacks in a simple inclusive concept: *i.e.*, as a matter of fact, only a portion of the receiver receives concentrated solar irradiance, to wit, part facing solar trough. However, this is exclusively dependent on rim angle of parabolic trough. Put differently, sun-facing portion of conventional and commercially available receivers not only are starved of concentrated solar radiation – but also, it do the adverse and the otherwise, *viz*. loosing gainful heat by radiation.

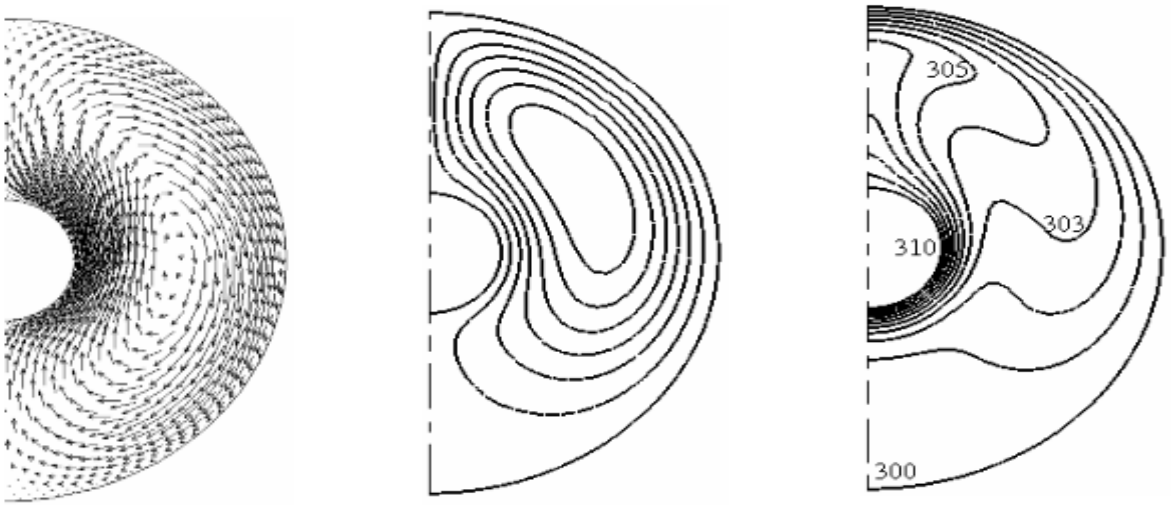

(a) **(b)** **(c)**

Figure 5.1 (a) velocity vector, (b) stream lines, and (c) isothermal zones of typical air filled PTC receiver annulus [Alshahrani et al., 2005]

Figure 5.2 demonstrates with numerical methodology of ANSYS FLUENT, the localised heating flux available to the absorber tube system pertaining to conventional air filled annulus which hinders for poor heat transfer and surplus losses.

Furthermore, two aforementioned problems with conventional receiver intensify and infuse together at higher temperature to form screaming big fat appallingly non-negotiable total heat losses (conduction and convection). To illustrate, at elevated temperatures, convection currents are so exaggeratedly amplified in terms of motion of currents (refer fig. 5.1 (a)) that the heat loss varies piecemeal in an over linear fashion as explained by fig. 5.3. In another words, with increase in temperature differences in bottom and above portion, heat loss per meter of the receiver is also increased in a linear fashion.

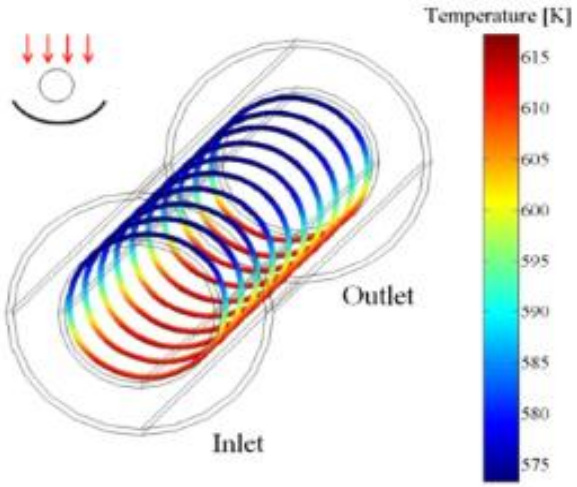

Figure 5.2 Temperature distribution or heat flux profile of a typical PTC absorber [Wang et al., 2014]

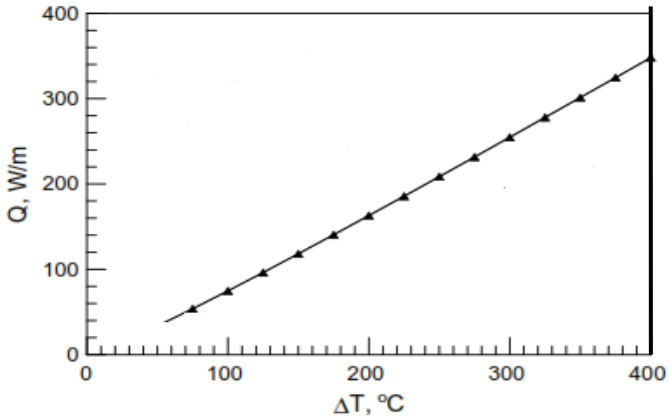

Figure 5.3 Heat losses from receiver having a linear relation with circumferential temperature difference [Al-Ansari et al., 2011]

Figure 5.4 predicts the probable among many likely solutions in which a heat insulating material is jibbed in the upper half portion of receiver to reduce buoyancy induced convection currents while limiting them to the lower half portion only. As a consequence of above design change, Absorber tube temperature is increased dramatically in contrast to the glass casing. This makes the air annulus practically stratify: keeping the hot air near the absorber and cooler air near the glass casing; to top it off – convection losses are reduced piecemeal, even in the lower half of annulus. In addition to convection loss reduction, radiation losses are also anticipated to be dropped, as upper face insulation reduces the surface glass enclosure temperature. Besides, contrasting the Achilles' heel of this design paradigm: firstly, some of the solar radiations are thwarted to reach the absorber which may effect to reduce the conversion efficiency in one form or another, secondly, taking a leaf out of work of Ansary et al. [2011]: Thermal performance of the altered receiver is reckoned to be degenerated at elevated temperatures. This deterioration is apparently on the account of increase in thermal conductivity of insulating material apropos increase in systems temperature, thus transgressing its inherent promise to allegiance.

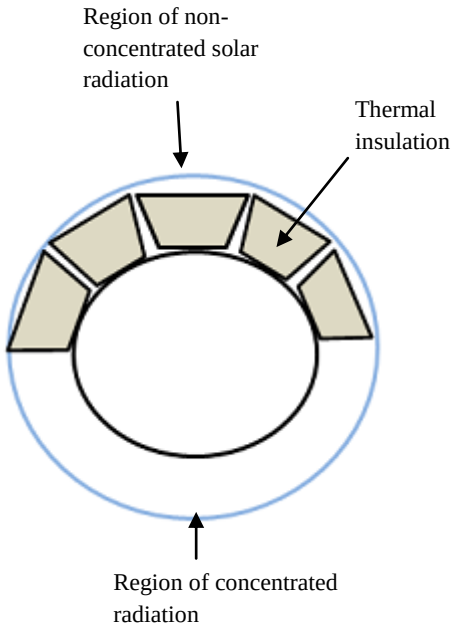

Figure 5.4 One side insulated receiver as the solution to the problem under investigation

In addition, Temperature distribution inside of solar receiver holds paramount importance for efficient heat conveying through heat transfer fluid (HTF). It is worthy to mention that, DNI, Inlet velocity and temperature of the HTF effects the temperature distribution in most substantial way. Long story short, it is observed that temperature distribution of heat transfer

fluid along with the absorber discretely varies radially. This is the case of localised heating of absorber in which highest temperature resides underneath or bottom side of it. The reason primarily belongs to non-symmetrical and inhomogeneous focusing of solar irradiance which is of greater intensity at bottom. Figure 5.5 (a) and fig. 5.5 (b) computationally imitates the working condition of typical receiver model with the practical conditions of DNI, wind speed, inlet temperature and velocity of HTF as 1200 W/m^2, 3 m/s, 450 K and 2 m/s respectively. Accordingly, it can be corroborated from fig. 5.5 (a) and fig. 55 (b) that fluid temperature in bottom portion is distinctively higher than the other half of it, which is in perfect agreement with Ya – Ling at al. [2010], who simulated the parabolic trough receiver for different geometric concentration and rim angles of parabolic trough collector.

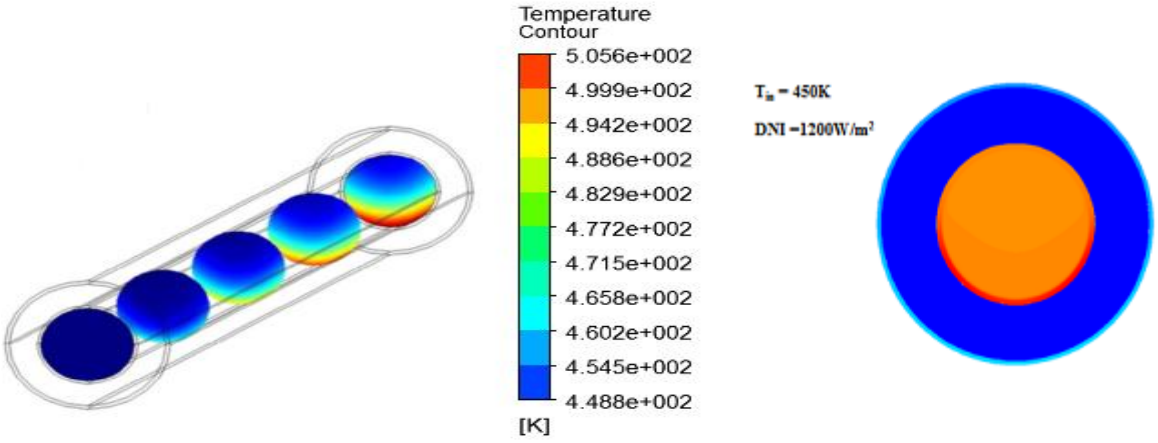

(a) **(b)**

Figure 5.5 Temperature distributions in (a) heat transfer fluid, and (b) in receiver

Bearing this in mind, this section will try to address the aforementioned shortcoming of the conventional air filled receiver *viz.*, localised heating of absorber and would try to simulate and numerically figure out whether the new design with one sided thermal insulation, actually works out the localized heating of absorber due to inhomogeneous solar irradiance in fluxing. In another words, this chapter serves to simulate and report the heat flux localisation of the conventional air filled receiver and would conceptually and figuratively contrast the predominant feature of one sided insulated receiver *i.e.* elimination of solar heat flux localization with the added reward of reduction in buoyancy induced convection currents as reported by Ansari et al. [2011]. This transformation from localised to holistic heat flux distribution is due to the one sided insulation, which binds the solar heat influx upcoming from the bottom side of receiver and enforces quarantine to the surrounding which previously

(in conventional air filled annulus receiver) was getting drained out. In addition to validation of aforementioned experimental findings, the scope of this chapter would also span out towards the relative comparison of convection losses due to different wind conditions and mass flow rate of HTF in both the receivers and finally try to markedly add contrast towards the usage of modified receiver in lieu of conventional one. For the above purpose, modified geometry of the one sided insulation is modelled in fluent module of ANSYS. In particular, glass wool is used for the purpose of insulation and the geometry was modelled in perfect agreement with the design of commercially available PTC receivers, more specifically, the current model is emulated with the one used in "1 MW power plant, based on solar parabolic trough collector, (PTC)," commissioned by, "National institute of solar energy, (NISE), India."

5.1 Physical model of modified receiver

Physical model as described by fig. 5.6 (a) is modelled in ANSYS module: design modeller, which perfectly emulates the practical working data given in Table 5.1 Figure 5.6(a), fig. 5.6(b) and fig. 5.6(c) illustratively demonstrates the heat interaction model, front view and isometric view of the current geometry. Absorber tube made of steel is placed concentric to the glass envelope. Whilst, air is filled in parabolic trough facing half annulus; Thermal insulation namely glass wool is filled in the other half. TherminolVp-1 is used as heat transfer fluid and is made to flow in the absorber, setting a chain of heat transfer processes in the whole receiver, fig. 5.6(a), as described by Ricardo et al. [2011], can be summed up as: concentrated solar irradiance focusing on lower part of receiver (q_{sol}), assimilation of solar irradiance transmitted by glass enclosure in the absorber through radiation ($q_{sol\text{-}abs.}$), heat transfer between absorber and heat transfer fluid (HTF) through convection ($q_{a,\ f\text{-}conv.}$), buoyancy induced convection heat transfer due to entrapped air in lower part of annulus ($q_{a\text{-}conv.}$), radiation and conduction heat losses through bottom part of glass envelop and absorber ($q_{g\text{-}rad.}$), ($q_{a\text{-}rad.}$), ($q_{a\text{-}cond.}$), lastly convention heat losses from glass tube to environment, ($q_{g\text{-}conv.}$). Conduction losses, for the time being, from the upper insulated portions are neglected as this is the inherent purpose of insulation for which it is employed for. These heat interaction schemes will be all together evaluated and worked upon for the current problem under investigation.

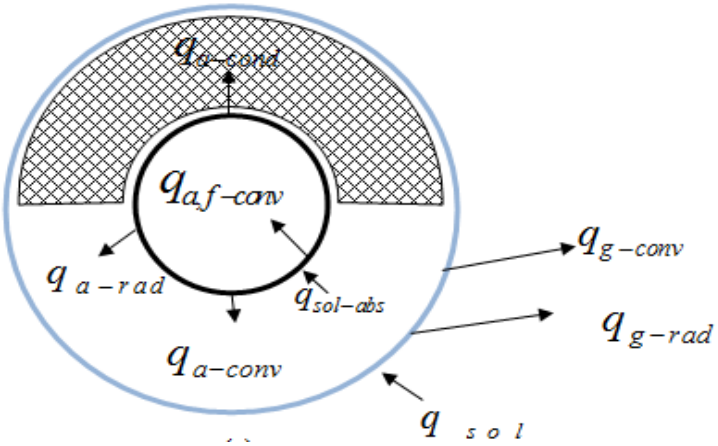

(a)

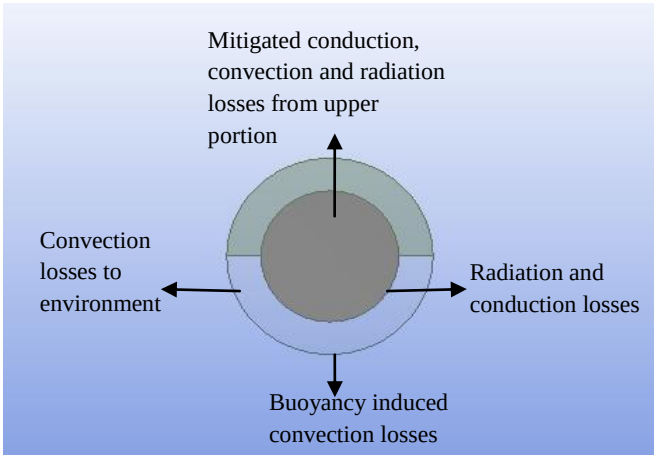

(b)

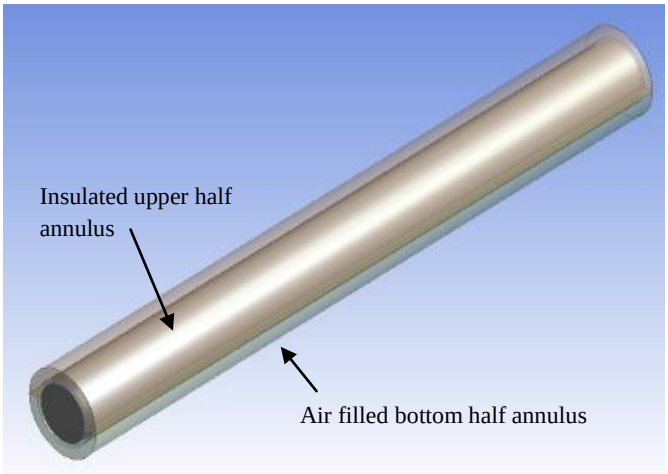

(c)

Figure 5.6 (a) Heat interaction model of current problem under investigation, configuration of modified receiver (b) front view, and (c) isometric view

Table 5.1: System specification of solar receiver

Aperture of single solar trough	136.25 m^2
Length of single trough	12.5 m
Aperture width	5.57 m
Aperture length	12.5 m
Outer diameter of absorber	0.0720 m
Inner diameter of absorber	0.0705 m
Outer diameter of glass envelop	0.1205 m
Inner diameter of glass envelop	0.1115 m
Absorber steel material	321-H stainless steel
Absorber glass material	Silicate glass
Rim angle	70^0
Concentration ratio	80

5.2 Heat transfer scheme from one-side insulated absorber

5.2.1 Absorber to heat transfer fluid (HTF)

Heat transfer from one-half insulated annulus as given by Recardo et al. [2011] on the assumptions of steady state incompressible flow and is given by the accompanying partial differential equation:

$$\frac{A}{2}\rho_f C_{p,f}\frac{dT_f}{dt} = -\dot{m}\frac{d}{dz}\left(C_{p,f}T_f + \frac{V_f^2}{2}\right) + \dot{Q}_{a,f-conv} \tag{5.1}$$

Where, heat transfer by convection, $Q_{a,\ f\text{-}conv.}$, is illustrated by the following equation and the Nusselt number is reckoned by correlation given by Schlunder et al. [1983] and Gnielinski et al. [200].

$$\dot{Q}_{a,f-conv} = \pi Nu_f k_f \left(T_a - T_f\right) \tag{5.2}$$

5.2.2 Buoyancy induced convective heat transfer from absorber to trapped air

Buoyancy induced convective heat transfer given by equation:

$$Q_{a-conv} = h_a \pi D_a \left(T_a - T_g\right) \tag{5.3}$$

Where, Coefficient of convective heat transfer (h_a) for annular space is reckoned by Dushman et al. [1962]

5.2.3. Heat transfer from glass envelope to environment

Mode of heat transfer from glass tube to environment is convection and radiation. Furthermore, two cases of convection losses exists namely, natural convection where wind velocity is assumed zero and forced convection with considerable wind velocity. For the current problem, particularly, convection losses with substantial wind velocity are investigated for which the following equation beholds.

$$Q_{g-conv} = h_g \pi D_g \left(T_g - T_\infty\right) \tag{5.4}$$

Where, convective heat transfer coefficient is calculated by the correlation given by Mullick et al. [1986]

$$h_w = 4V_w^{0.58} D_2^{-0.42} \tag{5.5}$$

5.3 Governing equations

Heat loss to surrounding occurs by convection and radiation, for current investigation, only convection losses for the described, modified industrial receiver would be considered. Mode of convection heat transfer, in particular, is contingent on wind conditions [Hongbo et al., 2015]. Following assumptions are presumed for the interest of model simplification.

- Radiation exchange in infrared spectrum amounts to zero.
- Thickness upon which solar influx comes about is very little compared to overall dimension hence absorption of solar irradiance at any level is strictly defined on solar flux terms and error associated it is minimal [Özisik et al., 1973] and [Modest et al., 2003]
- Pressure gradient is assumed small enough to make fluid in steady state and incompressible preconditions.
- Edges are assumed adiabatic adding up to zero end loss [Chengmu et al., 2014]
- The enclosure is infinitely long, put differently; flow is strictly assumed to be two dimensional.

Partial differential equation (PDE) governing this analytical model of turbulent flow inside absorber includes: continuity, momentum and energy. On the account of HTF and its velocity distribution, critical Reynolds number shoots higher than 4000 resulting in fluid flow in turbulent region, therefore employing k-ε turbulence model [Wilcox et al. 1998]. Following are the equations that govern the fluid flow:

- Equation for steady state condition and incompressible flow

$$\frac{\partial p}{\partial t} = \frac{\partial p}{\partial x} = \frac{\partial p}{\partial y} = \frac{\partial p}{\partial z} = 0 \tag{5.6}$$

- Continuity equation

$$\nabla . u_i = \frac{\partial u}{\partial x} + \frac{\partial v}{\partial y} + \frac{\partial w}{\partial z} = 0 \tag{5.7}$$

- Energy equation

$$\rho C_p u_i \frac{\partial T}{\partial x_i} = \left(k + k_T\right) \frac{\partial}{\partial x_i} \left(\frac{\partial T}{\partial x_i} \right) \tag{5.8}$$

- Momentum equation

$$\frac{\partial}{\partial t}(\rho u_i) + \nabla . (\rho u_i u_j) =$$
$$-\nabla p + \frac{\partial}{\partial x_j} \left[(\mu + \mu_t) \left(\frac{\partial u_i}{\partial x_j} + \frac{\partial u_j}{\partial x_i} \right) - \frac{2}{3} (\mu + \mu_t) \frac{\partial u_i}{dx_i} \delta_{ij} - \frac{2}{3} \rho k \delta_{ij} \right] + \rho g_i \tag{5.9}$$

Where k_T represents turbulent conductivity, k stands for thermal conductivity of fluid and μ_t is defined as turbulent viscosity, calculated by the correlation used by Wilcox et al. [1980]. Upon simplification and considering gravity in y direction, simplified momentum equation for steady state incompressible flow can be represented by following equations:

$$\rho(u \frac{\partial u}{\partial x} + v \frac{\partial u}{\partial y} + w \frac{\partial u}{\partial z}) = -\frac{\partial p}{\partial x} + (\mu + \mu_t) \left[\frac{\partial^2 u}{\partial x^2} + \frac{\partial^2 u}{\partial y^2} + \frac{\partial^2 u}{\partial z^2} \right] \tag{5.10}$$

$$\rho(u \frac{\partial v}{\partial x} + v \frac{\partial v}{\partial y} + w \frac{\partial v}{\partial z}) = -\frac{\partial p}{\partial y} + (\mu + \mu_t) \left[\frac{\partial^2 v}{\partial x^2} + \frac{\partial^2 v}{\partial y^2} + \frac{\partial^2 v}{\partial z^2} \right] + \rho g_y \tag{5.11}$$

$$\rho(u \frac{\partial w}{\partial x} + v \frac{\partial w}{\partial y} + w \frac{\partial w}{\partial z}) = -\frac{\partial p}{\partial z} + (\mu + \mu_t) \left[\frac{\partial^2 w}{\partial x^2} + \frac{\partial^2 w}{\partial y^2} + \frac{\partial^2 w}{\partial z^2} \right] \tag{5.12}$$

In addition to these primaries PDE, RNG k-ε; two equation model, to calculate turbulent energy dissipation (ε) and turbulent production (k) will be utilized. These equations are given underneath

$$\nabla . (\rho \varepsilon u_i) = (u + \frac{u_t}{\sigma_\varepsilon}) \nabla^2 \varepsilon + C_{1\varepsilon} \frac{\varepsilon}{k} (G_k + C_{3\varepsilon} G_b) - \rho C_{2\varepsilon} \frac{\varepsilon}{k} \tag{5.13}$$

$$\nabla . (\rho k u_i) = (u + \frac{u_t}{\sigma_k}) \nabla^2 k + G_k + G_b - \rho \varepsilon \tag{5.14}$$

Where, G_b and G_k represents kinetic energy generation owing to buoyancy effect and velocity gradient effect of turbulent flow respectively. C_ε and $C_{3\varepsilon}$ are RNG two equation constants equal to 1.420 and 1.680 respectively, μ_t is the eddy viscosity which is altered in RNG model on the account of swirl generation and is reckoned by correlation from Launder et al. [1974].

5.4 Boundary conditions

Boundary conditions are needed to be assigned prior to solve the current problem, these are detailed as below.

- Flow inlet and flow outlet boundary conditions:

  $V_{in} = u_{avg} = w = (V/\text{Across sectional})$;

  $u = v = 0$; $T=Tin$;

  [k_{in}=2%; μ_t=95] [Wilcox et al., 1980]

  Turbulence intensity calculated on basis of hydraulic diameter by the correlation of Wilcox et al. [1980].
- Pressure outlet boundary conditions: fully grown viscous flow [Tao., 2001]
- Wall boundary conditions: no slip condition with walls deemed as stationary. Since, heat transfer fluid used is TherminolVp-1, subsequently, k-ε model is adequate to be used in the near vicinage of solid liquid interface regions which are predominated by viscous effects over turbulent effects, in addition to this, to simulate real time problem of viscous effect near the vicinage of solid wall, standard logarithmic wall function are used as boundary conditions [Launder et al., 1974].
- Outer surface of absorber tube is subjected to be non-zero heat flux conditions. Incident solar flux is simulated as heat flux around the one-side insulated absorber tube [Cheng et al., 2010]. Solar heat flux around the one side insulated absorber is presumed to be constant.

5.5 Numerical method

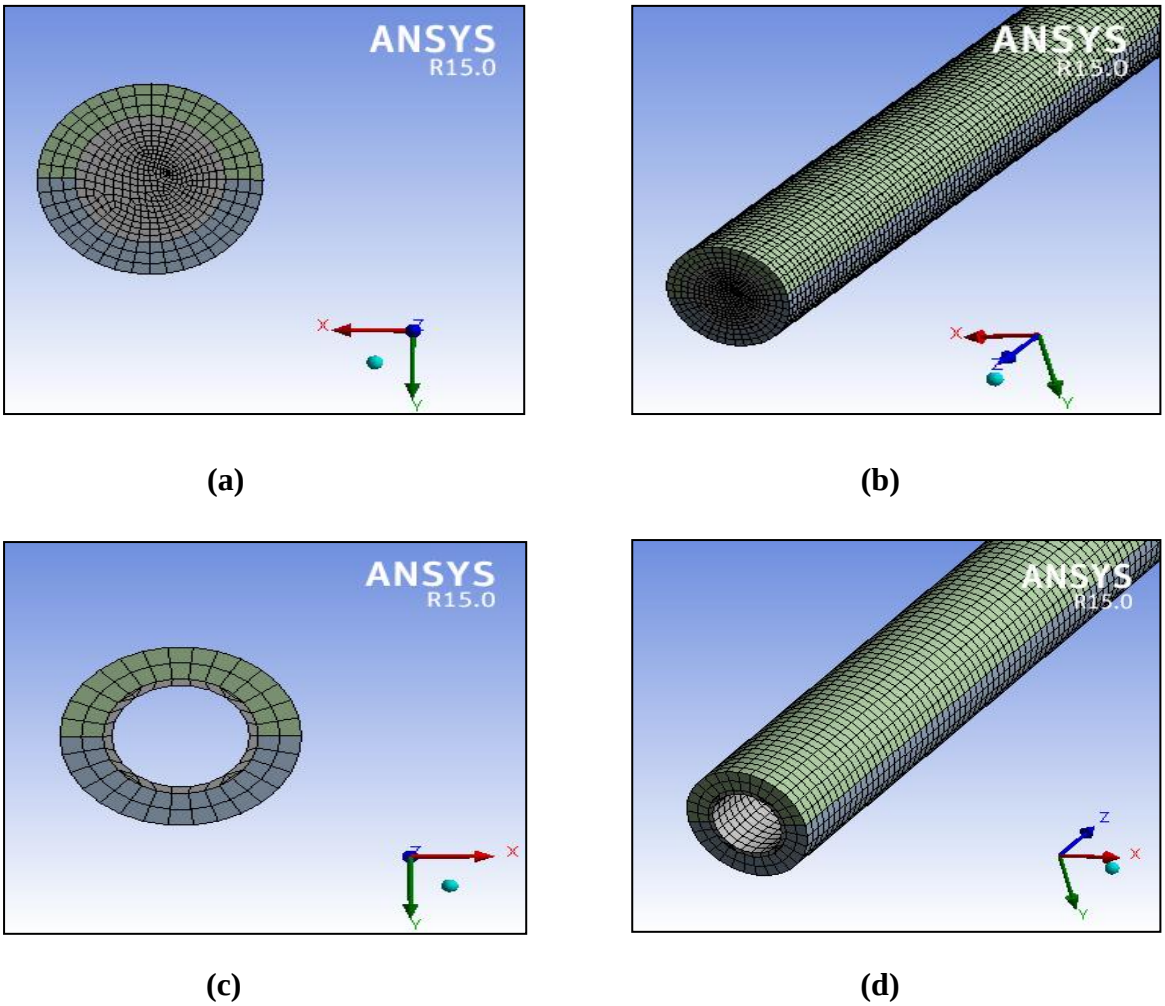

Figure 5.7 Grid generation for numerical simulation: (a) front view, and (b) isometric view of receiver tube respectively, (c) front view, and (d) isometric view of annulus respectively

Geometric data utilised for current modelling procedure is shown in Table 5.1. As soon as the model is modelled in ANSYS modeller of ANSYS academic version 15.0, its domains are allotted and fixed as solid or fluid, agreeing to their congenial nature to problem. It is then subsequently exported for meshing where it is discretised to finitude of smaller sub-elements. Figure 5.6(a) and fig. 5.6(b) demonstrate the front and isometric view grid generation for the four node quadrilateral face mesh throughout the cylinder volume. Grids are not spread out evenly over the whole computational zone rather they have higher compactness almost in the interior volume of domain. Figure 5.6(c) and fig.5.6(d) demonstrate the front and isometric view of meshed annulus incorporated and fitted with one side glass wool and other side air

PDE eq. (5.1) to eq. (5.14) are extremely coupled and nonlinear, therefore, numerical

approximation approach of CFD is used in which finite volume method is utilized to discretise these governing equations. Meanwhile, natural convection induced by temperature dependent properties of HTF (TherminolVp-1) are also accounted in momentum equation by introducing its density as a function of temperature (eq. (5.11)) and activating gravity in Fluent [Agustin et al., 2007]. To begin with, energy checkbox is turned on for ANSYS to solve heat transfer equations, followed by, k-ε framework, to ensure turbulent flow (eq. (5.13) and eq. (5.14)) in absorber. With applying the above mentioned boundary conditions in the appropriate and respective named selection, surface to surface (S2S) model is put to use to simulate heat transfer mechanism. Thermo physical properties of the different materials used are listed in Table 5.2. In addition, temperature dependent input properties of HTF and glass wool are assigned to polynomial correlation with temperature, agreeing to the data point curve fitting, and, are allotted in the respective user defined polynomial material properties in ANSYS fluent. In the same way, it should be remarked, that the heat transfer coefficient of the ambient air is reckoned by curve fitting [Burkholder et al., 2008], to represent the characteristics of wind speed ranging in 0.43 – 4.99 m/s. On the other hand, most importantly, recirculation inlet and recirculation outlet boundary conditions of icepack solver are invoked from fluent TUI command list to reckon the steady state temperature reach for the model under investigation.

Table 5.2: Thermo physical properties of material used

Material	k (W/m-K)	ρ (kg/m^3)	C_p (J/kg-k)	μ(kg/m-s)
TherminolVp-1	0.117	1068	2270	0.000457
Air	0.0242	1.125	1006.43	0.00001789
Glass wool	0.04	18	670	-
Silicate glass	1.4	2.5	840	-
Stainless steel	16	7920	444	-

CHAPTER 6

NUMERICAL VALIDATION & RESULTS AND DISCUSSIONS

This section uses the concept of heat transfer schemes, governing equations, meshed modelled geometry of the conventional and modified receiver to figuratively produce the circumferential temperature difference (CTD) or temperature distribution profile at different angular and longitudinal positions of both absorber tubes. Secondly, comparative heat loss in conventional and modified receiver at different longitudinal position would be demonstrated. Afterwards, validation of the experimental findings as discussed in chapter 4 would be accomplished.

6.1 Temperature analysis of problem under investigation

The consequent resultant simulation model is demonstrated graphically to render a clear perspective of temperature distribution round the circumference of absorber tube and the fluid. Figure 6.1 quintessentially illustrates the distinctive temperature profiles or isotherms of conventional air filled annulus receiver system and modified half air half glass wool annulus receiver system. To begin with, two set of temperature contours are measuredly shown here namely: temperature contour 1, depicting circumferential temperature profile of absorber, pertaining to conventional receiver and, temperature contour 2 demonstrating isotherms of absorber, pertaining to modified one side insulated receiver. Isotherms thus formed here for both the geometries are explicitly assigned here with the specified temperature range (refer fig. 6.1) and, the time taken by recirculating inlet and recirculating outlet boundary condition to reach the steady state temperature difference for that Peculiar condition. More specifically, to illustrate the gist, for a specific flow rate of HTF the inlet and outlet temperature difference is given against the time taken to achieve it and the temperature distribution around the absorber tube along with the fluid, for both the cases under the abovementioned boundary conditions. In another words, with a little research on the overleaf classified and distinctive pictorial representation of both the cases.

t (min)	ΔT(K)	Temperature Contour 1		ΔT(K)	Temperature Contour 2
2mins	25		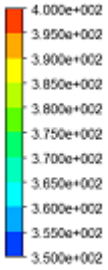	28	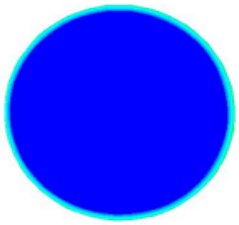
4mins	32.75	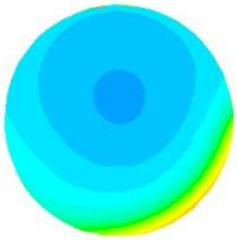	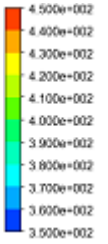	37.85	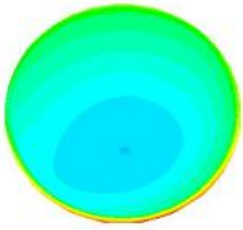
6mins	41.67	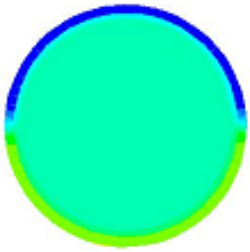	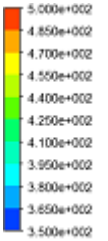	47.45	
8mins	52.78		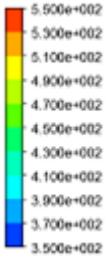	61.87	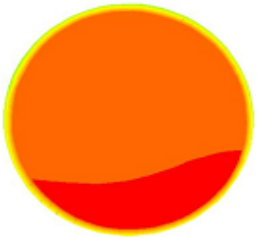
10mins	59.89		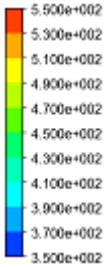	72.65	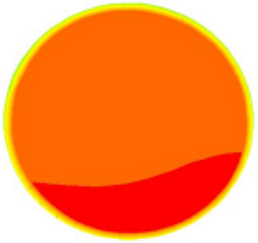

Figure 6.1 Isothermal zones of fluid flow in both absorbers along with surface temperature profile of absorber tube

It is apparently clear that for a particular mass flow rate of HTF that net positive temperature gain pertaining to modified receiver is higher in lieu to conventional one. Moreover, for conventional receiver, it can be concluded that the temperature of sun facing side of absorber is lower than the temperature of parabolic trough facing side; and this difference becomes even more prominent in the axial direction, this is apparently due to the fact that immense density of solar flux is concentrated in the lower part and the upper part is starved of the heating. This uneven heating of absorber may produce maximum temperature difference of as much as 110 K.

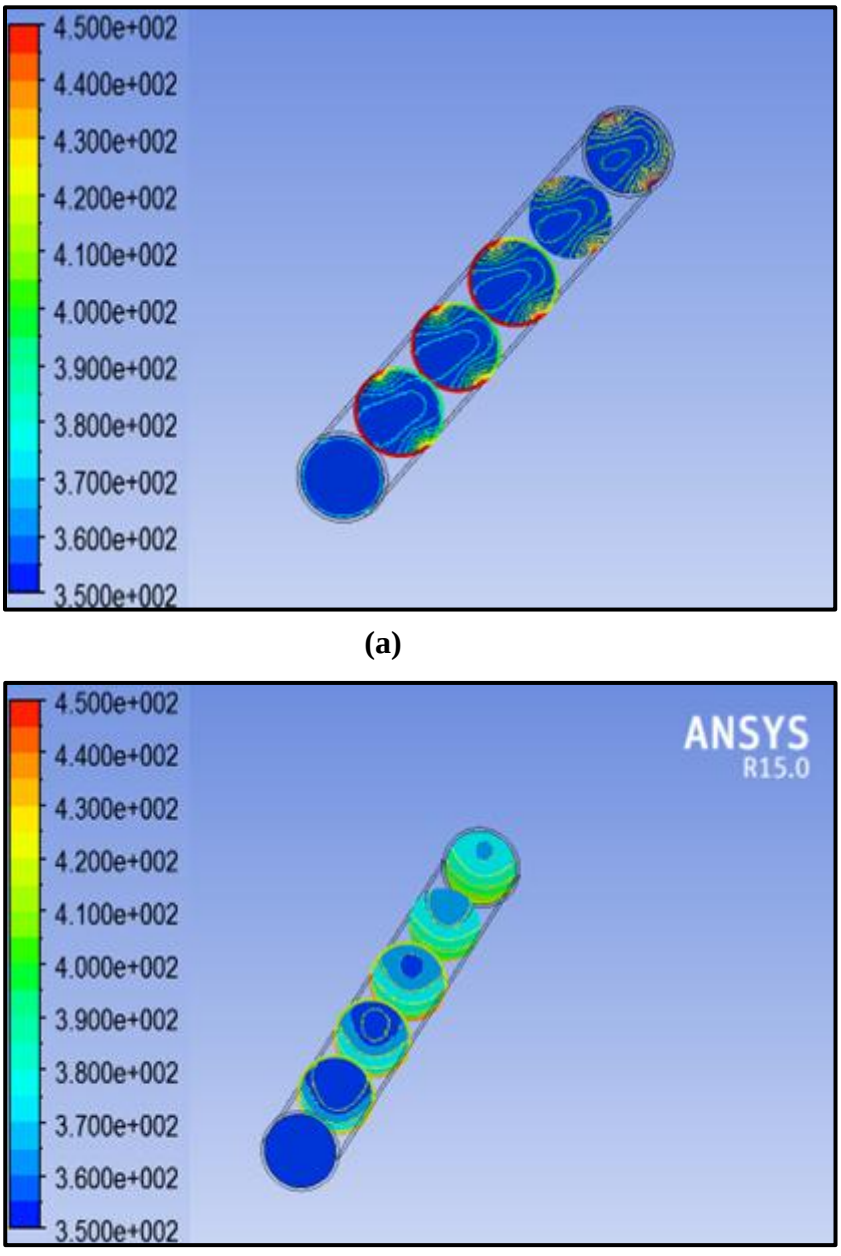

Figure 6.2 Cross – sectional temperature profile at different longitudinal section of (a) conventional receiver, and (b) modified receiver

Table 6.1: Simulated conditions

	DNI (W/m^2)	h_o (W/m^2k)	m (kg/s)	T_{in} (K)	T_{o1}(K)	T_{o2}(K)
Condition 1	950	10	0.8	350	300	300
Condition 2	1000	12.5	1	350	300	300
Condition 3	1050	13.5	1.2	350	300	300
Condition 4	1100	14	1.4	350	300	300

Figure 6.2 demonstrates the cross-sectional view of absorber tube at different longitudinal section and tries to illustrate the circumferential temperature distribution in axial direction for both the cases; this further corroborates the more symmetrical temperature profile of modified receiver in contrast to the conventional receiver. In addition, it is self – evident that the temperature of the upper part of modified absorber is also increased considerably (owing to reduction in conduction and convection losses) contrary to the conventional receiver which further stimulates the impetus for better temperature distribution and heat exchange mechanism from absorber tube to HTF.

6.2 Circumferential temperature difference of both receivers

To further illustrate, based on the above test conditions, it can be ensured that in case of conventional receiver, asymmetric heat flux around the absorber tube prevailingly varies circumferentially from as small as a few W/m^2 to the outmost 40 kW/m^2. This considerable heat flux variation is reduced up to a level of significance in case of modified receiver. Likewise, fig. 6.3(a) and fig. 6.4(b) primarily demonstrate the circumferential surface temperature variation for both the cases based on the aforementioned test conditions. To begin with, temperature is way higher at location $\varphi=180^0$ for both the cases in lieu of rest of other two prime locations viz. $\varphi = 0^0$ and $\varphi = 360^0$. The reason being $\varphi = 180^0$ lie on the parabolic trough facing side and the other two on the opposite sun facing side, while, $\varphi = 90^0$ lies in between. To quantify the syllogism of the two mentioned figures—it is apparently and logically inferred from both the graphs, that the magnitude of surface temperature variation or temperature distribution for both receivers is neither substantially equivalent nor similar in any spatial arrangement or size. While, for conventional receiver, temperature profile is more inclined and steeper in dispersion, in another words, there is an abrupt change in temperature in the radial location of $\varphi = 90^0$ to $\varphi = 180^0$ (refer fig. 6.3(a)). As a consequence, temperature

is distributed widely over full range of 420 – 550 K, in case of conventional receiver. Contrary to this, temperature distribution of modified receiver is more gradual, ranging from comparatively lower value of 460 – 500 K, (refer fig. 6.3(b)). To bear out, temperature dispersion graphs at various longitudinal locations is taken into account to gravitate the contrast in both the cases of receiver.

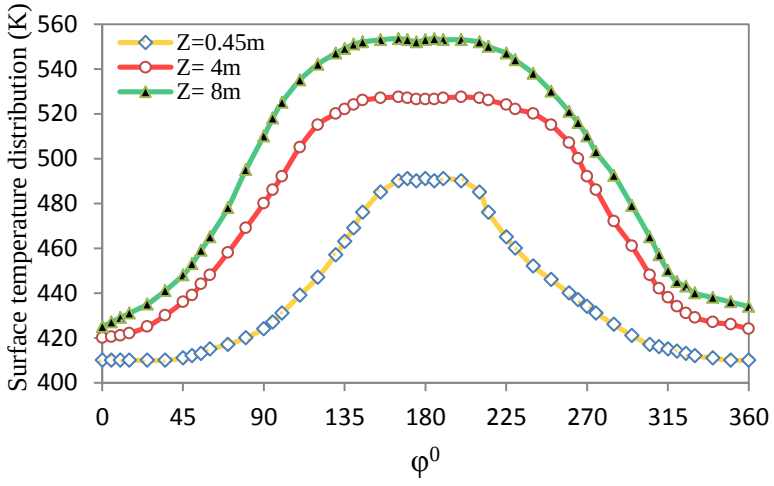

(a)

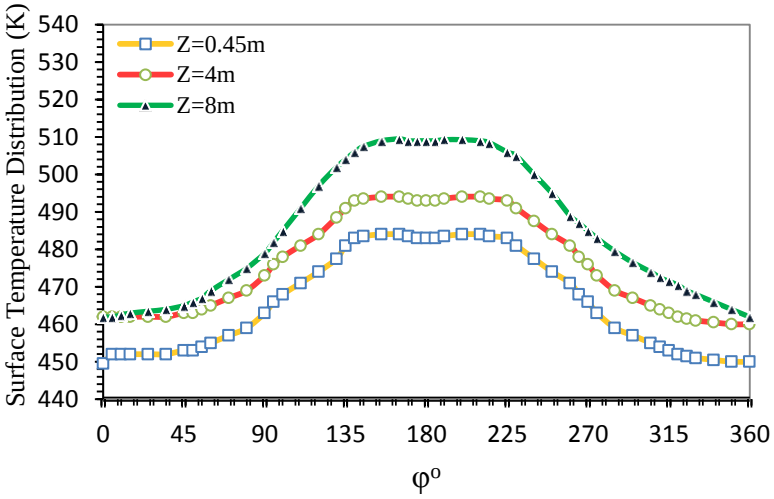

(b)

Figure 6.3 Temperature distribution profiles of (a) conventional receiver, and (b) modified receiver.

In addition to circumferential temperature change, temperature also changes longitudinally or in axial direction in a significant manner. Figure 6.4(a) and fig. 6.4(b) precisely and explicitly infer this longitudinal temperature distribution of absorber tube in radial direction and makes it apparently evident that temperature variation in modified receiver is far more favourable than conventional one. In another words, as we go along the absorber tube in longitudinal or

axial direction a maximum temperature difference of about 102 K is observed at the outlet of absorber tube *viz.*at x = 8 m. However, this temperature gradient is reduced substantially, up to almost 70 K in case of modified receiver.

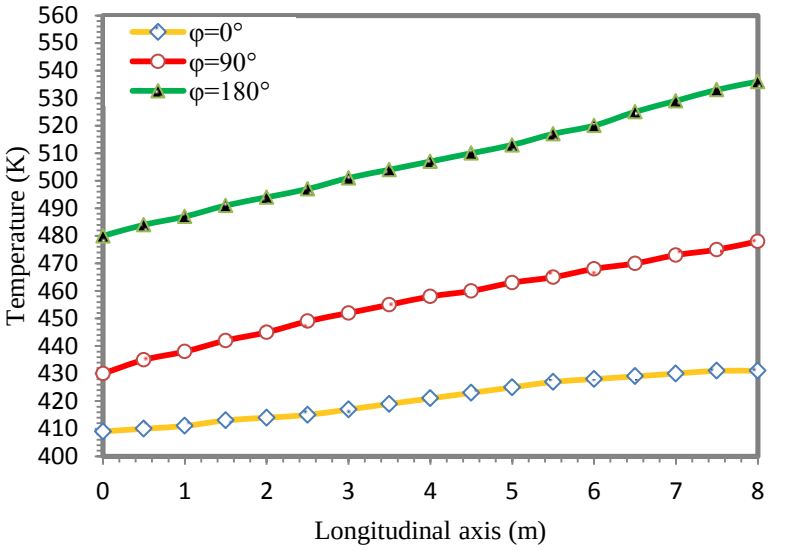

(a)

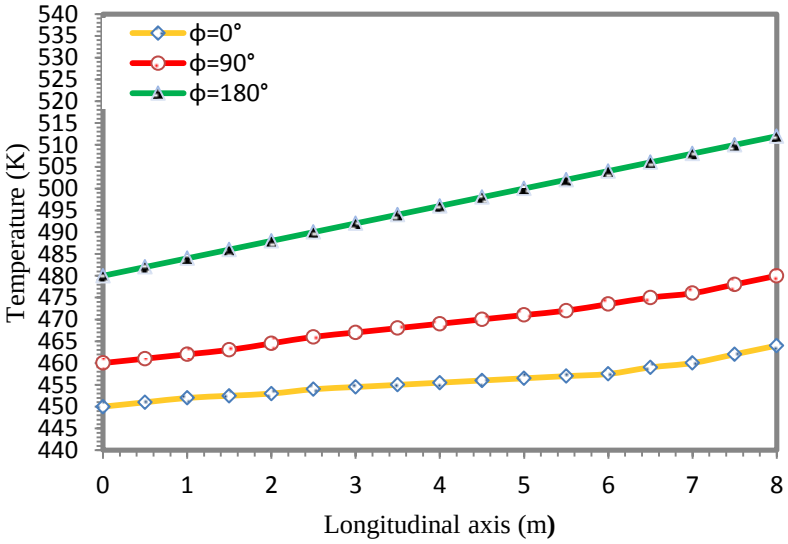

(b)

Figure 6.4 Temperature distribution profile along the length of the absorber for different circumferential location for (a) conventional receiver, and (b) modified receiver

6.3 Overall heat loss analysis of both receivers

Figure 6.5(a) and fig. 6.5(b) demonstrates the comparative heat loss between conventional and modified receiver, and in point of fact, heat loss by conduction in modified receiver is far significantly and noticeably lesser than analogous convection heat loss in a non – Insulated

conventional one. This fact is highly advocated for temperate temperature differences, while, at advanced temperature differences this level of significance is reduced due to escalation of thermal conductivity of glass wool dwindling its heat insulation properties (refer fig. 6.5 (a)).

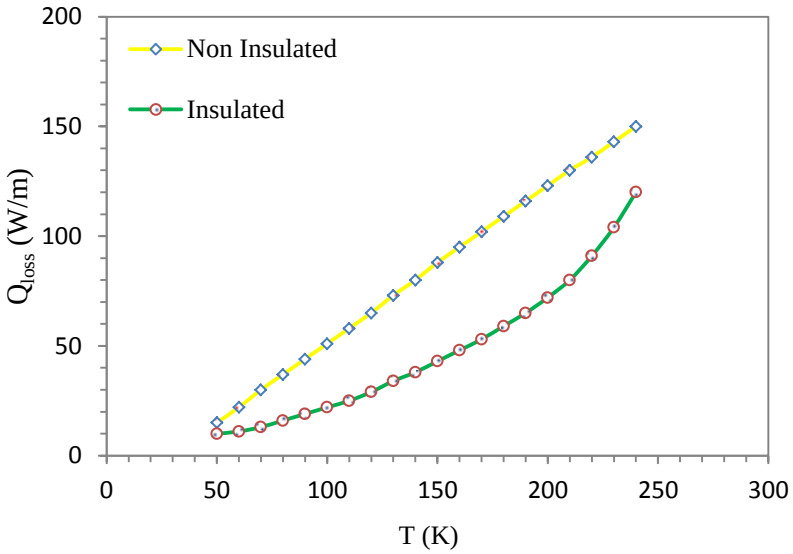

(a)

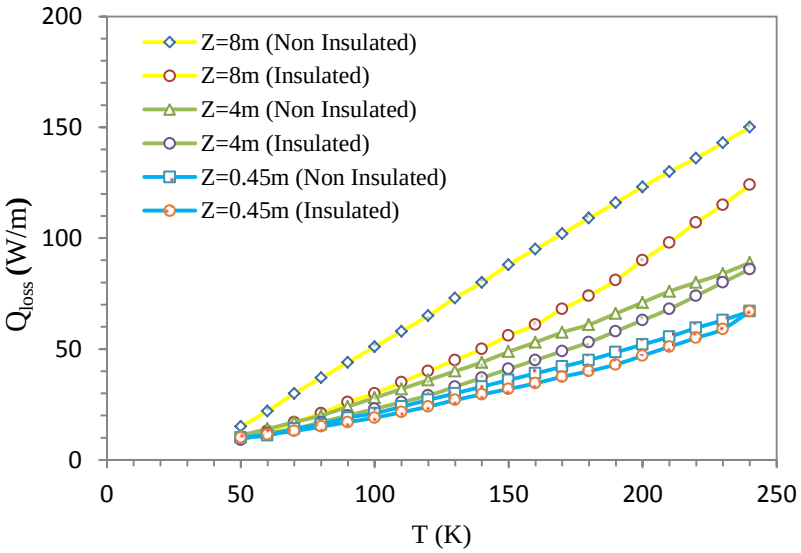

(b)

Figure 6.5 Comparative heat loss in (a) conventional and modified receives, and (b) for different longitudinal section

Additionally, this fact is further reinforced by fig. 6.4(b) which demonstrates heat loss in relation to different outlet temperature at separate longitudinal sections of both receivers. As a matter of fact, maximum heat loss reduction reported here is 28% when modified receiver was used.

6.4 Convective loss analysis

This section not only serves as the validation of the experimental results through ANSYS simulation but also tries to calculate the heat loss by convection through both the receivers and will graphically compare both, to give the direct contrast and to take receiver of the rails, as far as its performance is considered in comparison with conventional one.

In chapter 4 *i.e*. experimental findings, influence of mass flow rate was considered on different temperatures such as glass tube temperature, mean absorber temperature and outlet temperature. Correspondingly, in this section of ANSYS simulation, those results were numerically calculated by emulating and simulating the real time experimental conditions, applying boundary conditions and heat flow schemes as described in chapter 5. Results obtained were in perfect agreement to the experimental findings and for the sake of reproducibility of the same; those conditions were simulated for a good range of data obtained in experimentation. After temperature validation, convective heat transfer would be calculated for both the receivers and both would be compared graphically.

The influence of mass flow rate of HTF on the absorber tube temperature, glass tube temperature and outlet temperature for both receivers was studied and illustrated in the following Figure 6.5(a) and fig. 6.5(b). To begin with, outlet temperature and absorber temperature seems to be inversely proportional to mass flow rate, being to their lowest value against 1.2 kg/s of mass flow rate. As mass flow rate is further reduced, considerably from 1.2 kg/s to 0.6 kg/s, noticeable increase in both temperature takes place. Nevertheless, this noticeable temperature rise is marginally appreciated for the case of modified receiver (refer fig. 6.5(b)). Most of all, outlet temperature is also increased for a particular flow rate in case of modified receiver.

Glass tube temperature has a direct consequence on convection losses by natural convection from envelope. The reduction in glass tube temperature with wind velocity connotes escalation in convection losses across the glass tube. This fact is further corroborated by the calculated values of convective heat coefficient (refer Table 6.2) for the respective wind speed. Coefficient of convective heat transfer calculated here was computed by the relation developed by Mullick et al. [1989]. Accordingly, to quantify the convection losses, different wind velocities pertaining to the experimental circumstances were emulated and tabulated in Table 6.2, with their respective heat transfer coefficients. Temperatures T_1 and T_2 designate glass tube temperature of conventional and modified receiver at different mass flow rates of HTF. It is ostensibly clear that as the velocity of wind is augmented from 1

m/s to 4m/s; decrease in glass tube temperature follows for nearly both the mass flow rates of HTF.

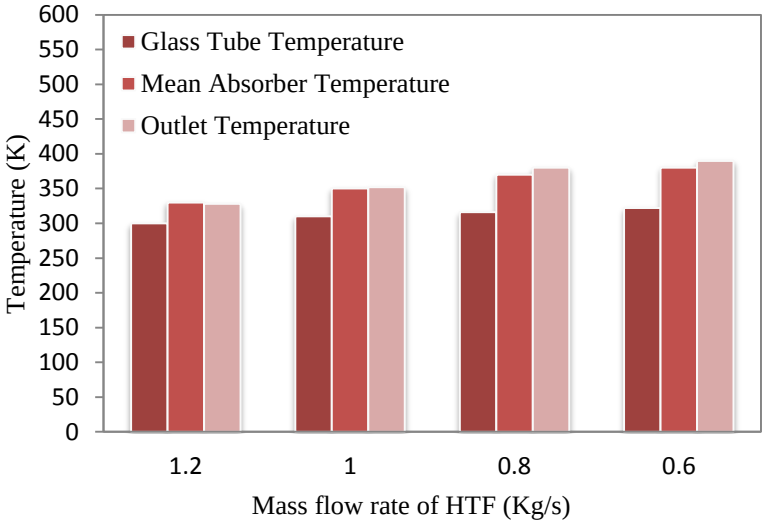

(a)

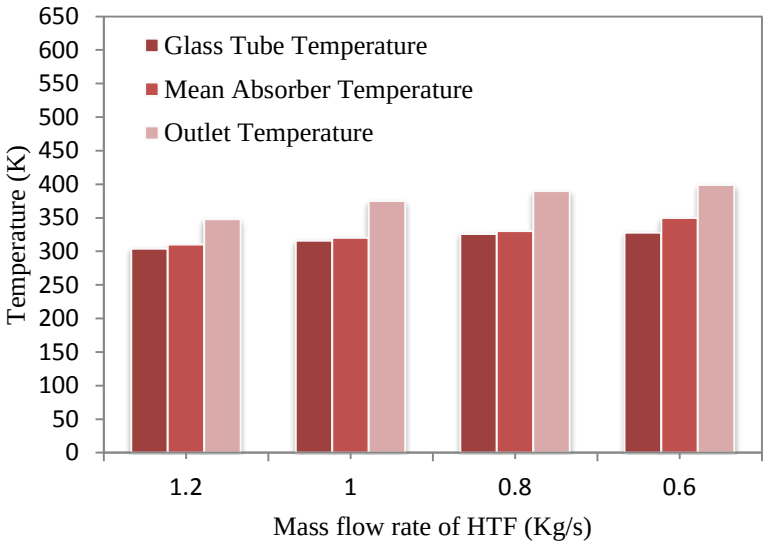

(b)

Figure 6.6 Temperature influence of mass flow rate on (a) conventional receiver, and (b) modified receiver.

A comparative stance is given in Table 6.2 which apparently suggests that for modified receiver, both glass tube temperature as well as its variation with wind speed is comparatively lower than the conventional one. This is also supported by the conventional heat loss against velocity of wind in fig. 6.7. Consequently, as wind speed is increased from 1 m/s to 4 m/s total heat loss by convection from conventional receiver is increased by 16.2%, for mass flow rate of 1.2 kg/s, on contrary, for the same mass flow rate convective losses are increased by a

comparative lower value of 12.5% in case of modified receiver. Same is the scenario with the lower mass flow rate (refer fig. 6.7).

Table 6.2: Direct influence of wind speed on glass tube temperature at different mass flow rate of HTF

Velocity of wind (m/s)	Convective heat transfer coefficient (W/m^2k)	Glass tube temp.T_1 (K) with mass flow rate of 1.2 kg/s	Glass tube temp. T_2 (K) with mass flow rate of 1.2 kg/s	Glass tube temp. T_1 (K) with mass flow rate of 0.8 kg/s	Glass tube temp. T_2 (K) with mass flow rate of 0.8 kg/s
1	9.72	338.58	337.56	340.02	339.12
1.5	11.9	336.23	335.59	337.85	336.85
2	13.75	334.84	333.45	336.46	335.42
2.5	15.38	332.12	330.81	333.78	332.25
3	16.85	330.89	329.54	332.52	331.42
3.5	18.20	328.93	327.62	330.53	329.49
4	19.45	328.23	327.32	329.64	327.85

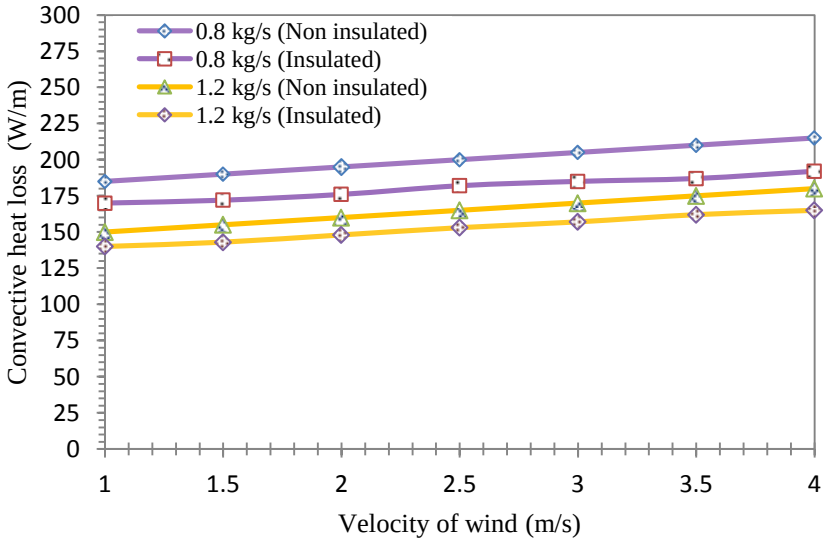

Figure 6.7 Influence of wind speed on convective heat loss for different mass flow rates

Table 6.2 and fig. 6.7 demonstrate the comprehensive model of heat loss by convection in relation to mass flow rate and wind velocity for both the conventional and modified receivers. In fact, the principal thermal loss that occurs in receiver is by radiation from absorber towards the glass enclosure; however, this space of the work is dedicatedly reserved towards the convection loss analysis of the modified receiver with one side insulation and outshines it from the conventional air filled annulus receiver. Nevertheless at the same time, losses by radiation are probable to be curtailed by using insulation in sun facing annulus as it confines the heat transfer in the near environ of absorber and impedes the augmentation of glass tube

temperature. Correspondingly, with palpable curtailment of convection losses, the usage of reformed receiver appreciably entails the radiation loss reduction as a logical consequence.

6.5 Model validation

For the purpose of code validation of numerical model, Results obtained from experimental investigation were compared with the simulation results and with the well documented case of experimental data performed in Sandia National Laboratories on LS-2 solar collector [Dudley et al., 1994]. In this experiment, tests were performed for various specifications, parameters of receiver and thermo – physical conditions such as vacuumed and aired annuli, varying sun shine, varying temperature range of receiver and heat transfer fluid and with varying heat transfer fluid itself such as water and Syltherm 800. However, for the sake of congeniality and suitability to the present model assessment and validation, a specific and relevant test results were referred and outlined in fig. 6.8. Test facility specification of Sandia National Laboratory's LS-2 solar parabolic collector is given in Table 6.3.

Figure 6.8 illustratively demonstrates the comparison between experimental model and simulated model for both insulated as well as non-insulated numerical model and both were paralleled and assessed with the previous documented case performed by Dudley et al. [1994]. This shows a clear agreement of experimental results and the simulated results of conventional receiver which furthermore is compared with the simulated data of modified receiver. Furthermore, for reproducibility, validation was performed for varying test conditions as given in Table 6.1. Also, from Fig. 6.8 it is apparently clear that the experimental data for convective loss is slightly higher than that of simulated model for non-insulated receiver; this might be due to the assumption of zero outer surface solar incidences in numerical model.

For numerical independency on grids, and to validate numerical simulation code, authentic and furnished case of wind condition with natural convection is simulated and compared with both cases. For the extant of numerical accuracy and veracity, and to ascertain the current model is grid insensitive, grid system examined by Cheng et al. [2010] is adopted and fairly high resolution is preferred. Simulations were iterated with varying number of nodes for the purpose of grid size tuning. Diverse meshing sets were adopted to solve the existing problem under investigation to study the influence of meshing and its sizing on solution. To illustrate, Table 6.4 predominantly demonstrates the grid size influence in radial course, in doing so, grid size are made to increase from (300 × 3145). As grid size is increased from this value to (350 × 3145), heat transfer difference is reduced from 3.48% to 0.59%, until it vanishes with

the grid size of (400 × 3145). Henceforth, the grid independency test is validated with grid sizing of (400 × 3145) for the current model.

Table 6.3: Specification of test facility at SEGS LS-2.

Facility size	7.8 x 5 m
Aperture area	39.2 m^2
Focal length	1.84 m
Outer diameter of absorber	0.07 m
Inner diameter of absorber	0.066 m
Outer diameter of glass envelop	1.15 m
Inner diameter of glass envelop	1.09 m
Rim angle	70^0
Concentration ratio	22.42
Glass material	Pyrex glass with
Transmittance of glass	0.95
Annulus condition	ambient air under 0.83 atm
Heat transfer fluid	Syltherm 800

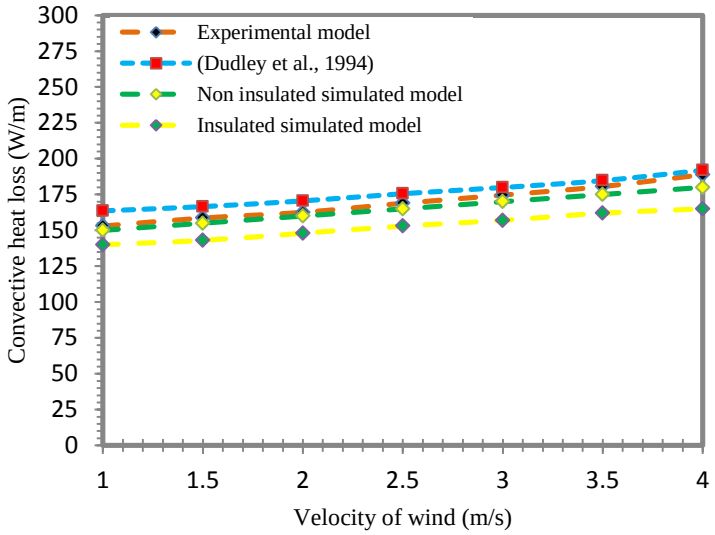

Figure 6.8. Comparison of proposed model with experimental data.

Table 6.4: Grid size and its effect on numerical problem under investigation.

Grid size	Q (W/m)	ΔQ/Q%
300 × 3145	148.112	3.48
350 × 3145	147.772	0.59
450 × 3145	147.683	0.01

CHAPTER 7

CONCLUSION AND FUTURE SCOPE OF WORK

7.1 Conclusion

En route to comparative thermal characteristics and temperature variations of parabolic trough receiver, numerical methodology of computational fluid dynamics was accessed. Regarding to the outmost congeniality to this paper, CFD approach was employed to computationally envision the lacuna in existing state of prevailing and mainstream air filled annulus receivers. Lacuna, as a consequence, pictured here includes: firstly, grave and appallingly unfavourable temperature distribution in absorber tube; due to non-symmetrical and in homogeneous attention of solar irradiance in the bottom trough facing part of receiver. Secondly, it includes buoyance induced convection losses due to air flanked in between annulus and lastly, natural wind prompted convection losses from glass tube. Though, radiation is considered to be biggest menace to thermal performance, the scope of the work was sternly confined to convection losses only. Regarding this, and as a consequence, heat transfer mechanism was simulated for the conventional receiver taking into account the impact of thermo-physical parameters of DNI, velocity of wind, mass flow rate etcetera.

Correspondingly, the probable solution in form of one side insulated receiver was simulated and the results were paralleled at every juncture. In addition, FLUENT module of ANSYS 15.0 was used for this simulation purpose. For this intention four experimental conditions were simulated over and the results were accredited with the grid independence test. A value-added covenant was observed between model under investigation and the simulated result. Temperature distribution, for further validation, was paralleled with the existing literature. More importantly, the conclusions predicted some splendid benefits of one side insulation in lieu of conventional receiver.

These outmatch performance of modified receiver in lieu of conventional receiver are enlisted below, these include:

- More uniform and homogeneous angular temperature distribution in absorber tube, resulted in better heat exchange process between absorber and HTF. This is also valid for longitudinal direction.

- A maximum of 28% reduction in overall heat loss when reformed receiver was used under the defined experimental and boundary conditions.
- Comparative figures of convective heat loss were estimated for both the receivers at different mass flow rate of HTF. This made the reformed receiver still again outmatch the conventional one with the fact of comparatively lower percentage of conventional loss increase (merely 12.5%) with increase in wind speed, compared with higher value of (17.2%) in case of conventional receiver.

For the sake of maxim – although, bottom half of receiver dotes sunlight; the other half abhors it. An off-limit redesign consideration in the form of insulated reformed receiver system for low temperature parabolic trough application was studied; entirely with the purpose to cater fundamental point of reference, that would promote the improvement of low temperature application PTC plants in India.

7.2 Future scope of work

Future scope of the work may include but is not limited to:

- This work is highly dedicated to the convectional loss arrest in air filled annuli receiver, these convection losses include buoyancy induced convection currents due to flanked air in annulus and convection losses due to wind speed. Correspondingly, a better '*avent-grade'* strategy of thermal insulation of non-concentrating side is used to curb those convection losses. However, with the foundation of the developed gist of this work it is apparently presumed that radiation losses might have been reduced due to glass tube temperature reduction with use of this thermal insulation. Nevertheless, the scope of this work is highly dedicated to convection loss analysis. Henceforth, radiation losses could be calculated in future.
- This work is done for the parabolic collector having rim angle of 70^0 for which it is predefined that half of receiver will receive concentrated solar influx while, other half will starve it. Henceforth, the results are highly specific and paralleled for parabolic trough collectors with rim angle of 70^0. With this as a source of muse, mathematical modelling could be carried out to calculate the span of receiver which would receive concentrated sun radiation for different rim angles of collector.

REFERENCES

Al-Ansari, H.; Zeitoun, O. (2011) Numerical study of conduction and convection heat losses from a half-insulated air-filled annulus of the receiver of a parabolic trough collector. *Solar Energy*, 85: 3036-3045.

Alguacil, M.; Prieto, C.; Rodriguez, A.; Lohr, J. (2014) Direct steam generation in parabolic trough collectors. *Energy Procedia*, 49: 21-29.

Antonelli, M.; Baccioli, A.; Francesconi, M.; Desideri, U. (2015) Electrical production of a small size concentrated solar power plant. *Renewable Energy*, 83: 1110-1118.

Arasu, A.V.; Sornakumar, T. (2007). Design, manufacture and testing of fibreglass reinforced parabolic trough for parabolic trough solar collector. *Solar Energy*, 81 (10): 1273-1279.

Alshahrani, D.; Zeitoun, O. (2005) Natural convection in air filled horizontal cylindrical annuli. *Alexandria Engineering Journal*, 44 (6): 813-823.

Barlev, D.; Vidu, R.; Stroeve, P.; (2011) Innovation in concentrated solar power. *Solar Energy Materials and Solar Cells*, 95: 2703-2725.

Cheng, Z.D.; He, Y.L.; Xiao, J.; Tao, Y.B.; Xu, R.J. (2010) Three-dimensional numerical study of heat transfer characteristics in the receiver tube of parabolic trough solar collector. *International Communications in Heat and Mass Transfer*, 37 (7): 782-787.

Delgado-Torres, A.M.; García-Rodríguez, L.; (2007) Comparison of solar technologies for driving a desalination system by means of an organic Rankine cycle. *Journal of Desalination*, 216: 276-291.

Dudley, V.; Kolb, G.; Sloan, M. (1994) Test results: SEGS LS2 solar collector. *Report of Sandia National Laboratories, Sandi*a, 94: 188-196.

Dushman, S. (1962) Scientific foundations of vacuum technique. Wiley: 2nd Ed, New York.

El Fadar, A.; Mimet, A.; Azzabakh, A.; Perez-Garci, M.; Castaing, J. (2009) Study of new solar absorption refrigeration powered by a parabolic trough collector. *Applied thermal Engineering*, 29: 1267-1270.

Egbo, G.; Sintali, I.S.; Dandakouta, H; (2014) Simulation of annular gap effect on performance of solar parabolic trough collector model TE38 in Bauchi. *American Journal of Engineering Research*, 12 (3): 102-108.

Feldhoff, J.F.; Benitez, D.; Eck, M.; Riffelmann, K. (2010) Economic potential of solar thermal power plants with direct steam generation compared with HTF plant. *Solar Energy*, 132: 4100-2010.

Fletcher, E.A. (2001) Solar thermal processing: a review. *Journal of Solar Energy Engineering, Transactions of ASME*, 123: 6-74.

Gnielinsli, V. (2009) Heat Transfer coefficients for turbulent flow in concentric annular ducts. *Heat Transfer Engineering*, 30 (6) 431-436.

Gharbi, N. El.; Derbal, H.; Bouaichaoui, S.; Said, N. (2011) A comparative study between parabolic trough collector and linear Fresnel reflector technologies. *Energy Procedia*, 6: 565-572

He, Y.; Xiao, J.; Cheng, Z.; Tao, Y. (2011) A MCRT and FVM coupled simulation method for energy conversion process in parabolic trough solar collector. *Renewable Energy*, 36: 976-985.

Islam, M.; Karim, A.; Saha, S.; Yarlagadda, P.K.D.V.; Miller, S.; Ullah, I. (2012) Visualization of thermal characteristics around the absorber tube of a standard parabolic trough thermal collector by 3D simulation. In the *proceedings of the 4th International Conference on Computational Methods*, Queensland university of technology, Gold Coast, Australia, 25-27 November: 202-216.

Kakat, S.; Shah, R.K.; Aung, W. (1987) Handbook of single-phase convective heat transfer. John Wiley & Sons .4th Ed, New York.

Karabulut, H. (2009) Construction and testing of a dish/Stirling solar energy unit. *Journal of the Energy Institute*, 82: 228-232.

Kuehn, T.H.; Goldstein, R.J. (1974) An experimental and theoretical study of natural convection in the annulus between horizontal concentric cylinders. *Journal of Fluid Mechanics*, 74 (4): 1847-1859.

Launder, B.E.; Spalding, D.B; (1974) The numerical computation of turbulent flows.

Computer Methods in Applied Mechanics and Engineering, 3: 269-289.

Liang, H.; You, S.; Zhang, H. (2015) Comparison of different heat transfer models for parabolic trough solar Collectors. *Applied Energy*, 148: 105-114.

Liu, C.; Mueller, W.K.; Landis, F. (1961) Natural convection heat transfer in long horizontal cylindrical annuli. *ASME International Developments in Heat Transfer*, 117: 976-984.

Liu, Q.; Yang, M.; Lei, J.; Jin, H.; Gao, Z.; Wang, Y. (2012) Modelling and optimizing parabolic trough solar collector systems using the least squares support vector machine method. *Solar Energy*, 86: 1973-1980.

Lobon, D.H.; Baglietto, E.; Valenzuela, L.; Zarza, E. (2014) Modelling direct steam generation in solar collectors with multiphase CFD. *Applied Energy*, 113: 1338-1348.

Mullick, S.C.; Nanda, S.K. (1989) An improved technique for computing the heat loss factor of a tubular absorber. *Solar Energy*, 42: 1-7

Marif, Y.; Benmoussa, H.; Bouguettaia, H.; Belhadj, M.; Zerrouki, M. (2014).Numerical simulation of solar parabolic trough collector performance in the Algeria Saharan region. *Energy Conversion and Management*, 85: 52-1529.

Mills, D.R.; Morrison, G.L. (2000) Compact linear Fresnel reflector solar thermal power plants. *Solar Energy*, 68: 263-283.

Modi, A.; Haglind, F. (2014) Performance analysis of a Kalina cycle for a central receiver solar thermal power plant with direct steam generation. *Thermal engineering*, 65: 2018-2014

Ozisik, M.N. (1973) Radiative transfer and interaction with conduction and convection. Wiley. 4th ed, New York.

Padilla, R.V.; Demirkaya, G.; Goswami, D.Y.; Stefanakos, E.; Rahman, M.M. (2011) Heat transfer analysis of parabolic trough solar receiver. *Applied Energy*, 88: 5097-5110.

Paetzold, J.; Cochard, S.; Vassallo, A.; Fletcher, D. F. (2014) Wind engineering analysis of parabolic trough solar collectors: the effects of varying the trough depth. *Journal of Wind engineering and industrial Aerodynamics*, 135: 118–128.

Schlunder, E.U. (1983) Heat exchanger design handbook. Hemisphere Publication

Corporation. 2nd Ed.

Siegel, R.; Howell, J.R. (1971). Thermal radiation heat transfer. McGraw-Hill. 3rdEd.

Sozen, A.; Altiparmak, D.; Usta, H. (2002) Development and testing of a prototype of absorption heat pump system operated by solar energy. *Applied Thermal Engineering*, 22: 1847-1859.

Steinmann, W.D.; Eck, M.; Laing, D. (2005) Solar thermal parabolic trough power plants with integrated storage capacity. *International Journal of Energy Technology and Policy*, 3 (1-2): 123-136.

Tao, W.Q. (2001) Numerical Heat Transfer. Xi'an Jiaotong University Press. 2nd Ed.

Tijani, A.S.; Roslan, A.M.S.B. (2014) Simulation analysis of thermal losses of parabolic trough solar collector in Malaysia using computational fluid dynamics. *Proceedings of Procedia Technology, 2nd International Conference on System-Integrated Intelligence: Challenges for Product and Production Engineering*, 15: 841-848.

Vignarooban, K.; Xinhai, Xu.; Arvay, A.; Hsu, K.; Kannam, A.M. (2015) Heat transfer fluids for concentrating solar power systems – A review. *Applied Energy*, 146: 383-396.

Wilcox, D.C., (1998) Turbulence modelling for CFD. DCW Industries Inc. 3rd Ed.

Wang, Y.; Liu, Q.; Lie, J.; Jin, H. (2015) Performance analysis of a parabolic trough solar collector with uniform solar flux conditions. *International Journal of Heat and Mass Transfer*, 82 : 236 -249.

Xu, C.; Chen, Z.; Li, M.; Zhang, P.; Ji, X.; Luo, X.; Liu, J. (2014) Research on the compensation of the end loss effect for parabolic trough solar collectors, *Applied Energy*, 115: 128-13.

Yaghoubi, M.; Ahmadi, F.; Bandehee, M. (2013) Analysis of heat losses of absorber tubes of parabolic through collector of Shiraz (Iran) solar power plant. *Journal of Clean Energy Technologies*, 1: 33-37.

Zemler, M.K.; Bohl, G.; Rios, O.; Boetcher, S.K.S. (2013) Numerical study of wind forces on parabolic solar collectors. *Renewable Energy*, 60: 498-505.

Zhang, L.; Yang, M.C.; Zhu, Y.Z.; Chen, H.J. (2015) Numerical study and optimization of

mirror gap effect on wind load on parabolic trough solar collector. *Energy Procedia*, 69: 233-241.

Web References:

W.1 1 MW solar thermal power plant, www.nise.res.in, (accessed on – 25/09/2015).

W.2 TherminolVp-1 heat transfer fluid, www.Easman.com, (accessed on – 12/10/2015).

W.3 Compact linear fresnal reflector, WWW.altan-solar.com, (accessed on – 05/11/2015)

APPENDIX

Table A1: Glass tube temperature at different wind velocities

Wind velocity (m/s)	Glass tube temp. at mass flow rate 1.4 kg/s of HTF	Glass tube temp. at mass flow rate 1.2 kg/s of HTF	Glass tube temp. at mass flow rate 1 kg/s of HTF	Glass tube temp. at mass flow rate 0.8 Kg/s of HTF
1	345.5	355	360.89	363.84
1.5	340	350.5	355.58	358.25
2	335	345	350.63	353.48
2.5	330.9	340	345.54	348.96
3	327.4	337	342.25	345.25
3.5	325.5	335.5	340.25	343.31
4	325.4	335	339.85	342

Table A2: Thermal efficiency for different wind velocities and inlet temperature

Wind velocity (m/s)	Thermal efficiency at inlet temp		
	T=180 ^{0}C	T=200 ^{0}C	T= 220 ^{0}C
0.2	35	32.33	30
0.4	37	34.25	32.33
0.6	39	36.23	34.5
0.8	40.5	38	36
1.00	42	39.5	37.5
1.2	43	40.5	38.5
1.4	43.5	41	39
1.6	43.8	41.5	39.5
1.8	44.2.	41.5	39.5

Table A3: Conventional receiver temperatures *vs.* mass flow rate

Mass flow rate (kg/s)	Glass tube temperature	Mean absorber temperature	Outlet temperature
0.6	322	380	390
0.8	316	370	380
1	310	350	352
1.2	300	330	328

Table A4: Modified Receiver temperatures *vs.* mass flow rate

Mass flow rate (kg/s)	Glass tube temperature	Mean absorber temperature	Outlet temperature
0.6	328	350	399
0.8	326	330	390
1	316	320	375
1.2	304	310	348

Table A5: Convective heat loss for varying wind velocity and mass flow rate of HTF

Wind velocity (m/s)	Convective heat loss with varying mass flow rate of HTF (W/m)			
	0.8 kg/sec		1.2 kg/s	
	Non insulated	Insulated	Non insulated	Insulated
1	185.52	170.45	150.26	140.89
1.5	190.56	172.26	155.25	143.82
2	195.25	176.45	160.53	148.23
2.5	200.23	182.78	165.54	153.69
3	205.26	185.27	170.36	157.45
3.5	210.89	187.36	175.27	162.12
4	215.85	192.96	180.96	165.92

Table A6: Heat loss *vs.* Circumferential Temperature difference for both receivers

Circumferential temperature difference (CTD)	Overall Heat loss in Non-insulated receiver (W/m)	Overall heat loss in insulated receiver (W/m)
50	15.23	10.65
60	22.56	11.60
70	30.25	13.23
80	37.12	16.36
90	44.89	19.69
100	51.89	22.26
110	58.47	25.16
120	65.96	29.19
130	73.36	34.95
140	80.23	38.93
150	88.01	43.78
160	95.89	48.73
170	102.65	53.37
180	109.89	59.45
190	116.45	65.57
200	123.78	72.25
210	130.45	80.83
220	136.54	91.94
230	143.12	104.26
240	160.32	120.20

Table A7: Heat loss for different longitudinal section of receiver

CTD	Overall heat loss for longitudinal distance of					
	Z=0.45m (Insulated)	Z=0.45 m (Non-insulated)	Z=4m (Insulated)	Z=4m (Non insulated)	Z=8m (Insulated)	Z=8m (Non insulated)
0	10	10.26	9.23	11.02	10.23	15.25
50	11.5	11.02	12.52	14.25	13.26	22.15

60	13	14.16	15.25	17.36	17.56	30.26
70	15	16.56	17.54	20.12	28.23	37.15
80	17	19.75	20.59	24.85	24.26	44.69
90	19	21.58	23.56	28.89	35.96	51.25
100	21.5	24.89	26.59	32.59	39.58	58.36
110	24	27.86	29.89	36.24	42.45	65.36
120	27	30.59	33.56	40.12	45.89	73.25
130	29.5	33.65	37.62	44.25	50.45	80.96
140	32.5	36.52	41.05	48.58	59.12	88.59
150	34.25	39.63	45.72	53.15	62.01	95.56
160	37.85	42.50	49.67	57.5	72.78	102.56
170	40.12	45.12	53.83	61.05	75.85	116.69
180	43.45	48.56	58.78	66.26	78.75	123.41
190	47.89	52.25	63.79	71.12	82.23	130.25
200	51.36	55.5	68.31	76.39	89.21	136.85
210	55.5	59.65	74.02	80.86	92.26	143.45
220	59	69.25	80.26	84.52	100.21	153.36